

# Finite-SNR Diversity–Multiplexing Tradeoff for Correlated Rayleigh and Rician MIMO Channels

Ravi Narasimhan, *Senior Member, IEEE*

**Abstract**—A nonasymptotic framework is presented to analyze the diversity–multiplexing tradeoff of a multiple-input–multiple-output (MIMO) wireless system at finite signal-to-noise ratios (SNRs). The target data rate at each SNR is proportional to the capacity of an additive white Gaussian noise (AWGN) channel with an array gain. The proportionality constant, which can be interpreted as a finite-SNR spatial multiplexing gain, dictates the sensitivity of the rate adaptation policy to SNR. The diversity gain as a function of SNR for a fixed multiplexing gain is defined by the negative slope of the outage probability versus SNR curve on a log-log scale. The finite-SNR diversity gain provides an estimate of the additional power required to decrease the outage probability by a target amount. For general MIMO systems, lower bounds on the outage probabilities in correlated Rayleigh fading and Rician fading are used to estimate the diversity gain as a function of multiplexing gain and SNR. In addition, exact diversity gain expressions are determined for orthogonal space–time block codes (OSTBC). Spatial correlation significantly lowers the achievable diversity gain at finite SNR when compared to high-SNR asymptotic values. The presence of line-of-sight (LOS) components in Rician fading yields diversity gains higher than high-SNR asymptotic values at some SNRs and multiplexing gains while resulting in diversity gains near zero for multiplexing gains larger than unity. Furthermore, as the multiplexing gain approaches zero, the normalized limiting diversity gain, which can be interpreted in terms of the wideband slope and the high-SNR slope of spectral efficiency, exhibits slow convergence with SNR to the high-SNR asymptotic value. This finite-SNR framework for the diversity–multiplexing tradeoff is useful in MIMO system design for realistic SNRs and propagation environments.

**Index Terms**—Finite signal-to-noise ratio (SNR), multiple antennas, outage probability, random matrices.

## I. INTRODUCTION

THE benefits of multiple antennas at both the transmitter and the receiver in a wireless link consist of increased reliability as well as high data rates. Techniques such as space–time coding [1] are primarily concerned with increasing reliability through spatial diversity, while spatial multiplexing [2], [3] achieves high data rates by using the spatial degrees of freedom to transmit independent data streams. For a particular transmission scheme, the conventional definition of diversity gain refers to the slope as the signal-to-noise ratio (SNR) tends to infinity of the error rate versus SNR curve for the *ideal*

channel conditions of independent and identically distributed (i.i.d.) Rayleigh fading. With this asymptotic definition of diversity, full-rank space–time codes ensure maximal spatial diversity [1]. In practice, however, the SNR is often sufficiently low such that the *effective* diversity, measured by the slope of the error rate versus SNR at a particular point, is significantly less than the slope at high SNR. This behavior is further exacerbated for multiple-input–multiple-output (MIMO) channels with a high-spatial correlation or line-of-sight (LOS) component, propagation conditions that are frequently encountered in practice.

In addition to exploiting the available spatial degrees of freedom, MIMO wireless systems typically employ rate adaptation algorithms based on the average received SNR. The level of rate adaptation, related to the multiplexing gain, must be selected for optimal performance at a given SNR. In this context, the following question is of interest: how does the error rate change for a change in the received SNR, given a certain rate adaptation strategy?

In order to address this question, it is necessary to characterize the behavior of the error probability as a function of the rate adaptation parameters. Fundamentally, this characterization involves the tradeoff between diversity and multiplexing in MIMO systems. Such a tradeoff was obtained in [4], which provides a framework to bridge the two extremes of pure diversity gain, related to link reliability, and pure multiplexing gain, related to spectral efficiency. The diversity–multiplexing tradeoff curve of a given space–time code enables one to determine the set of diversity and multiplexing gains that can be obtained simultaneously. This tradeoff was obtained as the SNR approaches infinity for i.i.d. Rayleigh-fading channels. The asymptotic characterization is typically valid for high data rates and correspondingly low error rates.

Systems such as wireless local area networks (WLANs) have moderate target packet error rates (PERs) around  $10^{-2}$ – $10^{-1}$  [5]. Furthermore, the SNRs encountered are usually in the range 3–20 dB. In addition, the wireless channel often exhibits high spatial correlation and may contain LOS components. Several recent papers [6]–[9] have noted that codes designed for maximum performance at high SNR in i.i.d. Rayleigh-fading channels are not optimal at low to medium SNR, especially in the presence of correlated fading. In such situations, asymptotic theory for high SNR and i.i.d. Rayleigh channels yields optimistic results. Thus, it is essential to characterize the diversity–multiplexing tradeoff for realistic SNRs, data rates, PERs, and nonideal fading channels.

This paper presents a nonasymptotic, finite-SNR analysis of the diversity–multiplexing tradeoff in MIMO systems for

Manuscript received September 19, 2005; revised March 1, 2006. The material in this paper was presented in part at the IEEE Globecom, St. Louis, MO, November 2005.

The author is with the Department of Electrical Engineering, University of California, Santa Cruz, CA 95064 USA (e-mail: ravi@soe.ucsc.edu).

Communicated by M. Médard, Associate Editor for Communications.

Digital Object Identifier 10.1109/TIT.2006.880057

realistic propagation conditions. The two cases of spatially correlated Rayleigh fading at either the transmitter or receiver and Rician fading are considered. Furthermore, no channel-state information (CSI) is assumed at the transmitter. The finite-SNR framework, necessary to evaluate the impact of these nonideal propagation conditions, is derived for quasistatic channels, such as those encountered in WLANs. In quasi-static fading, the channel is constant over one coding block, or packet, and varies independently across packets. Codes that approach capacity, such as turbo codes [10] or low-density parity-check (LDPC) codes [11], [12], are typically used on each packet such that the PER is well approximated by the channel outage probability. The outage probability is the probability that the mutual information, conditioned on the fading realization, between the transmitted and received signals is less than the target spectral efficiency. Based on the outage probability of MIMO systems, new definitions of diversity and multiplexing gains as functions of SNR are presented. The multiplexing gain is the ratio of the spectral efficiency at each SNR to the capacity of an additive white Gaussian noise (AWGN) channel with an array gain. For a constant multiplexing gain, the diversity gain is the negative slope of the outage probability versus SNR curve on a log-log scale.

Although there exist closed-form expressions for the moment generating and characteristic functions of the MIMO mutual information [13], [14], closed-form solutions for the cumulative distribution function (cdf), needed for the outage probability, are not tractable. Exact numerical computation of the cdf, which involves determinants of matrices of hypergeometric functions, provides little insight into the finite-SNR diversity–multiplexing tradeoff. Thus, a lower bound on the MIMO outage probability is derived to obtain an estimate of the diversity gain as a function of the multiplexing gain and SNR. This estimate is conservative in that the exact diversity gain is typically lower. The special case of orthogonal space–time block codes (OSTBC) is also considered since closed-form expressions for the outage probability are available. For spatially correlated Rayleigh fading, the achievable diversity gains at realistic SNRs are significantly lower than the high-SNR asymptotic values. For Rician fading, the maximum diversity gain is not always achieved at zero multiplexing gain. In fact, the diversity gain at some SNRs and multiplexing gains in Rician fading is larger than the asymptotic value for i.i.d. Rayleigh fading. These qualitative characteristics demonstrate the usefulness of the finite-SNR analysis described in this paper.

The remainder of the paper is organized as follows. Section II introduces the system model and the definitions of diversity and multiplexing gains as functions of SNR. Lower bounds on the outage probability are derived in Section III for the cases of spatially correlated Rayleigh fading and Rician fading. From these bounds, the diversity gain is estimated as a function of the multiplexing gain and SNR. Exact diversity gain expressions are computed for the case of OSTBC in Section IV. Section V presents outage probability and diversity gain curves at finite SNRs for various system and propagation conditions. Comparisons are also provided with high-SNR asymptotic results in the literature. A discussion of the finite-SNR results and interpretations of the limiting diversity gain as the multiplexing gain

approaches zero are given in Section VI. Conclusions are given in Section VII.

## II. SYSTEM MODEL AND DEFINITIONS

Consider a narrowband MIMO system with  $M_T$  transmit and  $M_R$  receive antennas. Let  $\mathbf{H}$  denote the  $M_R \times M_T$  channel matrix. For the case of correlated Rayleigh fading, correlation at the transmitter is assumed in this paper, although the results are easily applied to the case of receive antenna correlation. With transmit antenna correlation, the channel matrix can be written as  $\mathbf{H} = \mathbf{H}_w \mathbf{R}_T^{1/2}$ , where  $\mathbf{R}_T$  denotes the  $M_T \times M_T$  transmit covariance matrix and  $\mathbf{H}_w$  is a  $M_R \times M_T$  matrix whose elements are i.i.d. complex Gaussian random variables with zero mean and unit variance [15]. For the case of Rician fading, the channel matrix can be written as  $\mathbf{H} = \mathbf{H}_{\text{LOS}} + \mathbf{H}_{\text{NLOS}}$ , where  $\mathbf{H}_{\text{LOS}}$  and  $\mathbf{H}_{\text{NLOS}}$  denote the line-of-sight (LOS) and non-line-of-sight (NLOS) matrices, respectively. Frequently used models for these matrices are  $\mathbf{H}_{\text{LOS}} = \sqrt{K/(K+1)} \mathbf{1}_{M_R \times M_T}$  and  $\mathbf{H}_{\text{NLOS}} = (1/\sqrt{K+1}) \mathbf{H}_w$ , where  $K$  denotes the Rician  $K$ -factor,  $\mathbf{1}_{M_R \times M_T}$  denotes the  $M_R \times M_T$  matrix of all ones, and no spatial correlation is assumed [15]. Note that the rank-deficient LOS matrix arises in the usual case where the antenna separations at the transmitter and receiver arrays are much smaller than the range, or distance between transmitter and receiver. For simplicity, the phases of the LOS component are chosen such that the transmitter and receiver are in the broadside orientation. Diagonal phase matrices are needed to account for general array orientations. It can be shown that an arbitrary diagonal receive phase matrix does not affect the diversity–multiplexing tradeoff. Furthermore, if the transmit array orientation is known, a diagonal transmit phase matrix can be compensated for by adjusting the transmit antenna phases. Let  $\mathbf{x}$  and  $\mathbf{y}$  denote the transmitted and received vectors, respectively. The MIMO system equation is given by

$$\mathbf{y} = \mathbf{H}\mathbf{x} + \mathbf{n} \quad (1)$$

where  $\mathbf{n}$  is a complex AWGN vector with covariance  $N_0 \mathbf{I}_{M_R}$ , and  $\mathbf{I}_{M_R}$  denotes the  $M_R \times M_R$  identity matrix.

Under the assumption of quasistatic fading with capacity-achieving codes per packet, the PER is equal to the outage probability. With this model, the conventional asymptotic definitions of multiplexing and diversity gains of a MIMO system are given as follows [4]:

$$r_{\text{asymptotic}} = \lim_{\rho \rightarrow \infty} \frac{R}{\log_2 \rho} \quad (2)$$

$$d_{\text{asymptotic}} = - \lim_{\rho \rightarrow \infty} \frac{\log_2 P_{\text{out}}}{\log_2 \rho} \quad (3)$$

where  $r_{\text{asymptotic}}$  and  $d_{\text{asymptotic}}$  are the asymptotic multiplexing and diversity gains, respectively,  $R$  is the spectral efficiency (in bits per second/Hertz) of the MIMO system,  $\rho$  is the average SNR per receive antenna, and  $P_{\text{out}}$  is the outage probability. These definitions capture the *high-SNR* tradeoff of data rate (represented by the multiplexing gain) and reliability (represented by the diversity gain).

The need to characterize the diversity–multiplexing tradeoff at realistic SNRs, data rates, and PERs motivates the new fi-

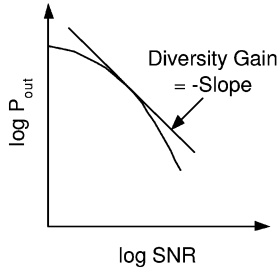


Fig. 1. Illustration of diversity gain at finite SNR.

nite-SNR definitions introduced in this paper. The multiplexing gain  $r$  is defined as the ratio of  $R$  to the capacity of an AWGN channel at SNR  $\rho$  with array gain  $g$ :

$$r = \frac{R}{\log_2(1 + g\rho)}. \quad (4)$$

The array gain is chosen by considering the MIMO mutual information  $I$  at low SNR. In the limit  $\rho \rightarrow 0$ ,  $I \approx \log_2(1 + \frac{\rho}{M_T} \|\mathbf{H}\|_F^2)$ , where  $\|\mathbf{H}\|_F$  is the Frobenius norm of the channel matrix  $\mathbf{H}$  [15]. Thus, for a fair comparison of diversity and outage performance across different  $M_T$  and  $M_R$  at low to medium SNRs, the array gain  $g$  is chosen such that  $g = \frac{1}{M_T} E[\|\mathbf{H}\|_F^2] = M_R$ .

Note that for a constant multiplexing gain  $r$ , the spectral efficiency increases as the SNR increases. The multiplexing gain  $r$  provides an indication of the sensitivity of a rate adaptation strategy as the SNR changes. As the value of  $r$  increases, a more sensitive rate adaptation strategy is used in which a moderate change in SNR can result in a significant change in the data rate.

As illustrated in Fig. 1, the diversity gain  $d(r, \rho)$  of a rate-adaptive system with a fixed multiplexing gain  $r$  at SNR  $\rho$  is defined by the negative slope of the log-log plot of outage probability versus SNR

$$\begin{aligned} d(r, \rho) &= -\frac{\partial \ln P_{\text{out}}(r, \rho)}{\partial \ln \rho} \\ &= -\rho \frac{\partial \ln P_{\text{out}}(r, \rho)}{\partial \rho} \end{aligned} \quad (5)$$

where  $P_{\text{out}}(r, \rho)$ , the outage probability of the MIMO link as a function of the multiplexing gain and SNR, is given by

$$P_{\text{out}}(r, \rho) = \Pr[I < r \log_2(1 + g\rho)]. \quad (6)$$

The significance of Definition (5) is that the diversity gain at a particular SNR can be used to estimate the additional SNR required to decrease the PER by a specified amount for a given multiplexing gain. The finite-SNR diversity gain (5) is well suited to a perturbation analysis of the MIMO system around a specified SNR. For large deviations, the behavior of the outage probability itself can be analyzed using (6).

### III. OUTAGE PROBABILITY AND DIVERSITY GAIN

In this section, lower bounds on the outage probability are computed for rate-adaptive MIMO systems under spatially correlated Rayleigh fading and Rician fading. The lower bounds

are then used to estimate the finite-SNR diversity gain using (5). The asymptotic diversity gain at high SNR is also computed.

The lower bounds on the outage probability are computed under the assumption of no CSI at the transmitter and perfect CSI at the receiver. In this case, equal power is allocated to each of the  $M_T$  transmit antennas. Thus, the MIMO mutual information conditioned on the channel realization  $\mathbf{H}$  is given by [16]

$$I = \log_2 \det \left( \mathbf{I}_{M_T} + \frac{\rho}{M_T} \mathbf{H}^* \mathbf{H} \right) \quad (7)$$

where the superscript  $*$  denotes conjugate transposition. For simplicity, it is assumed that  $M_R \geq M_T$  in this paper, although the results are easily generalized to arbitrary  $M_T$  and  $M_R$ .

#### A. Lower Bound on Outage Probability: Correlated Rayleigh Fading

A lower bound on the outage probability is now derived for Rayleigh fading with a possibly rank-deficient transmit covariance matrix  $\mathbf{R}_T$ . A rank-deficient transmit covariance matrix can arise with pinhole channels in which the transmitted signals have to reach the receiver through a small number of pinholes [17]. For a rank-one covariance matrix, there is only one path to link the scattering clusters at the transmitter and receiver. This situation can occur, for example, when signals have to go through windows in buildings. Other conditions that give rise to rank-one covariance matrices include zero angle spread or nonzero angle spread with all paths fading coherently [18].

Let  $0 < \mu_1 \leq \mu_2 \leq \dots \leq \mu_{N_T}$  denote the nonzero eigenvalues of  $\mathbf{R}_T$ , where the rank of  $\mathbf{R}_T$  is  $N_T \leq M_T$ . Furthermore, let a complex  $m \times m$  Wishart matrix  $\mathbf{A}$  with  $n$  degrees of freedom and covariance matrix  $\Sigma$  be denoted by  $\mathbf{A} \sim \mathcal{W}_m(n, \Sigma)$ . Note that  $\mathbf{A} \sim \mathcal{W}_m(n, \Sigma)$  if  $\mathbf{A} = \mathbf{G}^* \mathbf{G}$ , where  $\mathbf{G}$  is a  $n \times m$  matrix ( $n \geq m$ ) of zero-mean independent complex Gaussian row vectors with covariance matrix  $\Sigma$  [19], [20]. With these definitions, the mutual information has the following equivalent statistical representation.

*Lemma 1:* The mutual information  $I_{\text{corr}}$  for correlated Rayleigh fading is equivalent in distribution to the following:

$$I_{\text{corr}} \sim \log_2 \prod_{l=1}^{N_T} \left( 1 + \frac{\rho}{M_T} \lambda_{\text{corr},l} \right) \quad (8)$$

where  $\sim$  denotes “equivalent in distribution,”  $\lambda_{\text{corr},1} \leq \lambda_{\text{corr},2} \leq \dots \leq \lambda_{\text{corr},N_T}$  are the sorted eigenvalues of the complex Wishart matrix  $\mathbf{A}_{\text{corr}} \sim \mathcal{W}_{N_T}(M_R, \mathbf{D}_T)$ , and  $\mathbf{D}_T = \text{diag}(\mu_1, \mu_2, \dots, \mu_{N_T})$  is a diagonal matrix.

*Proof:* The proof is given in Appendix I.  $\square$

The outage probability of the rate-adaptive MIMO system can be expressed using (6) and (8) as follows:

$$\begin{aligned} P_{\text{out,corr}}(r, \rho) &= \Pr \left[ \log_2 \prod_{l=1}^{N_T} \left( 1 + \frac{\rho}{M_T} \lambda_{\text{corr},l} \right) < r \log_2(1 + g\rho) \right] \end{aligned} \quad (9)$$

where  $g = M_R$ . To derive a lower bound on  $P_{\text{out,corr}}(r, \rho)$ , the following lemma is used.

*Lemma 2:* For Rayleigh fading with transmit antenna correlation

$$\Pr[\lambda_{\text{corr},l} < x_l, l = 1, 2, \dots, N_T] \geq \Pr\left[\sum_{n=1}^l T_n < x_l, l = 1, 2, \dots, N_T\right] \quad (10)$$

where  $0 < x_1 < x_2 < \dots < x_{N_T}$  and  $T_n$  are independent random variables. The variables  $T_l$  can be written as

$$T_l = \sum_{n=1}^l G_{n,l} \quad (11)$$

where  $G_{n,l}$  are independent gamma random variables with parameters  $(\zeta_{n,l}, \eta_{n,l})$  and

$$\zeta_{n,l} = \begin{cases} 1, & n = 1, 2, \dots, l-1 \\ M_R - N_T + l, & n = l \end{cases} \quad (12)$$

$$\eta_{n,l} = \mu_n, \quad n = 1, 2, \dots, l. \quad (13)$$

*Proof:* The proof is given in Appendix II.  $\square$

Note that from [21], [22], the cdf of  $T_l$  can be written as a single gamma series

$$F_{T_l}(x) = \prod_{n=1}^l \left(\frac{\mu_1}{\mu_n}\right)^{\zeta_{n,l}} \times \sum_{k=0}^{\infty} \frac{\delta_{k,l} \gamma(M_R - N_T + 2l - 1 + k, x/\mu_1)}{\Gamma(M_R - N_T + 2l - 1 + k)} \quad (14)$$

where  $\gamma(m, x) = \int_0^x t^{m-1} e^{-t} dt$  is the incomplete gamma function and

$$\delta_{0,l} = 1$$

$$\delta_{k+1,l} = \frac{1}{k+1} \sum_{i=1}^{k+1} \left[ \sum_{j=1}^l \zeta_{j,l} \left(1 - \frac{\mu_1}{\mu_j}\right)^i \right] \delta_{k+1-i,l}, \quad k = 0, 1, \dots \quad (15)$$

For the case of i.i.d. Rayleigh fading,  $\mathbf{R}_T = \mathbf{I}_{M_T}$ . Thus, from (11)–(13),  $T_l$  becomes a gamma random variable with parameters  $(M_R - M_T + 2l - 1, 1)$  and has the cdf

$$F_{T_l}(x) = \frac{\gamma(M_R - M_T + 2l - 1, x)}{\Gamma(M_R - M_T + 2l - 1)}. \quad (16)$$

A lower bound on the outage probability is given in the following theorem.

*Theorem 1:* For Rayleigh fading,

$$P_{\text{out,corr}}(r, \rho) > \prod_{l=1}^{N_T} F_{T_l}(\alpha_{\rho,l}) \quad (17)$$

where  $r = \sum_{l=1}^{N_T} a_l$ ,  $a_0 = 0$ ,  $\alpha_{\rho,l} = \frac{M_T}{\rho} [(1 + g\rho)^{a_l} - (1 + g\rho)^{a_{l-1}}]$ , and  $F_{T_l}(\cdot)$  is given by (14) for the case of transmit

antenna correlation and by (16) for the case of no spatial correlation.

*Proof:* From (9) and the fact that  $(1 + g\rho)^r = \prod_{l=1}^{N_T} (1 + g\rho)^{a_l}$ , the lower bound on  $P_{\text{out,corr}}(r, \rho)$  is obtained as follows:

$$P_{\text{out,corr}}(r, \rho) = \Pr\left[\prod_{l=1}^{N_T} \left(1 + \frac{\rho}{M_T} \lambda_{\text{corr},l}\right) < \prod_{l=1}^{N_T} (1 + g\rho)^{a_l}\right] \quad (18)$$

$$\geq \Pr\left[\left(1 + \frac{\rho}{M_T} \lambda_{\text{corr},l}\right) < (1 + g\rho)^{a_l}, l = 1, 2, \dots, N_T\right] \quad (19)$$

$$\geq \Pr\left[1 + \frac{\rho}{M_T} \sum_{n=1}^l T_n < (1 + g\rho)^{a_l}, l = 1, 2, \dots, N_T\right] \quad (20)$$

$$> \Pr\left[T_l < \frac{M_T}{\rho} ((1 + g\rho)^{a_l} - (1 + g\rho)^{a_{l-1}}), l = 1, 2, \dots, N_T\right] \quad (21)$$

$$= \prod_{l=1}^{N_T} F_{T_l}(\alpha_{\rho,l}). \quad (22)$$

Inequality (19) follows from the fact that for any positive set of numbers  $u_l, v_l, l = 1, 2, \dots, N_T$ , we have  $u_l < v_l, l = 1, 2, \dots, N_T \Rightarrow \prod_{l=1}^{N_T} u_l < \prod_{l=1}^{N_T} v_l$ . Next, (20) follows from Lemma 2, and (21) is derived using the observation that

$$1 + \frac{\rho}{M_T} \sum_{n=1}^l T_n = 1 + \frac{\rho}{M_T} \sum_{n=1}^{l-1} T_n + \frac{\rho}{M_T} T_l < (1 + g\rho)^{a_{l-1}} + \frac{\rho}{M_T} T_l. \quad (23)$$

Finally, (22) follows from the independence of  $T_l, l = 1, 2, \dots, N_T$ .  $\square$

To obtain accurate diversity gains at finite SNR, the lower bound (17) is maximized over the exponents  $\{a_l\}$  for each  $r$  and  $\rho$ . The feasible set  $\mathcal{A}_r$  for  $\{a_l\}$  is determined by the fact that  $\alpha_{\rho,l} > 0$ . This constraint leads to the requirement  $a_l > a_{l-1}, l = 1, 2, \dots, N_T$ . From the conditions  $r = \sum_{l=1}^{N_T} a_l$  and  $a_0 = 0$ ,  $\mathcal{A}_r$  is given by

$$\mathcal{A}_r = \left\{ (a_1, a_2, \dots, a_{N_T}) \left| a_{l-1} < a_l < \frac{r - \sum_{k=1}^{l-1} a_k}{N_T - l + 1}, l = 1, 2, \dots, N_T - 1; a_{N_T} = r - \sum_{k=1}^{N_T-1} a_k \right. \right\}. \quad (24)$$

There exist efficient nonlinear programming techniques, such as variations of Newton's method [23] or sequential quadratic programming [24], to determine the vector  $(a_1, a_2, \dots, a_{M_T}) \in$

$\mathcal{A}_r$  that maximizes the right hand side of (17). The initial condition for the optimization is chosen as follows:

$$a_l^{(0)} = \begin{cases} \frac{r}{2N_T}, & l = 1 \\ \frac{1}{2} \left[ a_{l-1}^{(0)} + \frac{r - \sum_{k=1}^{l-1} a_k^{(0)}}{N_T - l + 1} \right], & l = 2, 3, \dots, N_T - 1 \\ r - \sum_{k=1}^{N_T-1} a_k^{(0)}, & l = N_T. \end{cases} \quad (25)$$

The computation time for the optimization is much smaller than Monte Carlo simulations for the exact outage probability. Furthermore, even without the maximization step, the analytical form of the lower bound (17) provides useful insight that cannot be obtained from simulations.

**B. Lower Bound on Outage Probability: Rician Fading**

In this section, a lower bound on the outage probability for Rician fading is derived. The derivation is based on results for noncentral Wishart matrices. In order to use these results, the Rician channel matrix must be modified by applying fixed unitary transformations at the transmitter. Specifically, let the vector of information symbols to be transmitted be denoted by  $\mathbf{s}$ . Let  $\mathbf{F}_{M_T}$  denote the  $M_T$ -point discrete Fourier transform (DFT) matrix whose elements are  $(\mathbf{F}_{M_T})_{k,n} = e^{-j2\pi kn/M_T} / \sqrt{M_T}$ ,  $k, n = 0, 1, \dots, M_T - 1$ . Let  $\mathbf{P}_{M_T}$  be the  $M_T \times M_T$  permutation matrix given by

$$\mathbf{P}_{M_T} = \begin{bmatrix} 0 & \dots & 0 & 1 \\ 1 & 0 & \dots & 0 \\ & \ddots & & \vdots \\ 0 & \dots & 1 & 0 \end{bmatrix}. \quad (26)$$

With these definitions, the transmitted vector is given by

$$\mathbf{x} = \mathbf{F}_{M_T} \mathbf{P}_{M_T} \mathbf{s}. \quad (27)$$

Under these unitary transformations, the equivalent channel matrix is given by

$$\mathbf{H}_{\text{eq}} = \mathbf{H}_{\text{LOS}} \mathbf{F}_{M_T} \mathbf{P}_{M_T} + \mathbf{H}_{\text{NLOS}} \mathbf{F}_{M_T} \mathbf{P}_{M_T} \quad (28)$$

$$= \sqrt{\frac{KM_T}{K+1}} \begin{bmatrix} \mathbf{0}_{M_R \times (M_T-1)} & \mathbf{1}_{M_R \times 1} \end{bmatrix} + \frac{1}{\sqrt{K+1}} \tilde{\mathbf{H}}_w \quad (29)$$

$$\equiv \tilde{\mathbf{H}}_{\text{LOS}} + \frac{1}{\sqrt{K+1}} \tilde{\mathbf{H}}_w \quad (30)$$

where  $\mathbf{0}_{M_R \times (M_T-1)}$  denotes the  $M_R \times (M_T - 1)$  matrix of all zeros and  $\tilde{\mathbf{H}}_w$  is an i.i.d. complex Gaussian matrix equivalent in distribution to  $\mathbf{H}_w$ .

Let a complex  $m \times m$  noncentral Wishart matrix  $\mathbf{A}$  with  $n$  degrees of freedom ( $n \geq m$ ), covariance matrix  $\mathbf{\Sigma}$ , and matrix of noncentrality parameters  $\mathbf{\Omega} = \mathbf{\Sigma}^{-1} \mathbf{M}^* \mathbf{M}$  be denoted by  $\mathbf{A} \sim \mathcal{W}'_m(n, \mathbf{\Sigma}, \mathbf{\Omega})$ . Note that  $\mathbf{A} \sim \mathcal{W}'_m(n, \mathbf{\Sigma}, \mathbf{\Omega})$  if  $\mathbf{A} =$

$\mathbf{G}^* \mathbf{G}$ , where  $\mathbf{G}$  is a  $n \times m$  matrix of independent complex Gaussian row vectors with covariance matrix  $\mathbf{\Sigma}$  and  $E[\mathbf{G}] = \mathbf{M}$ . As in the case of correlated Rayleigh fading, it can be shown that the mutual information  $I_{\text{Rice}}$  in Rician fading is equivalent in distribution to the following:

$$I_{\text{Rice}} \sim \log_2 \prod_{l=1}^{M_T} \left( 1 + \frac{\rho}{M_T} \lambda_{\text{Rice},l} \right) \quad (31)$$

where  $\lambda_{\text{Rice},1} \leq \lambda_{\text{Rice},2} \leq \dots \leq \lambda_{\text{Rice},M_T}$  are the sorted eigenvalues of the complex noncentral Wishart matrix  $\mathbf{A}_{\text{Rice}} \sim \mathcal{W}'_{M_T}(M_R, \frac{1}{K+1} \mathbf{I}_{M_T}, (K+1) \tilde{\mathbf{H}}_{\text{LOS}}^* \tilde{\mathbf{H}}_{\text{LOS}})$ .

Similar to Lemma 2, the following lemma is introduced.

*Lemma 3:* For Rician fading

$$\Pr[\lambda_{\text{Rice},l} < x_l, l = 1, 2, \dots, M_T] \geq \Pr \left[ \sum_{n=1}^l X_n < x_l, l = 1, 2, \dots, M_T \right] \quad (32)$$

where  $0 < x_1 < x_2 < \dots < x_{M_T}$  and  $X_n$  are independent random variables. For  $l = 1, 2, \dots, M_T - 1$ ,  $X_l$  are gamma variables with parameters  $(M_R - M_T + 2l - 1, 1/(K+1))$ , and  $X_{M_T}$  is a noncentral gamma variable with shape parameter  $M_R + M_T - 1$ , noncentrality parameter  $K M_R M_T$ , and scale parameter  $1/(K+1)$ . The cdf of  $X_l$  is given by (33) shown at the bottom of the page.

*Proof:* The proof is given in Appendix III.  $\square$

A lower bound on the outage probability  $P_{\text{out,Rice}}(r, \rho)$  is derived using Lemma 3, as given in the following theorem. The proof is similar to the Proof of Theorem 1 and, hence, is omitted.

*Theorem 2:* For Rician fading

$$P_{\text{out,Rice}}(r, \rho) > \prod_{l=1}^{M_T} F_{X_l}(\tilde{\alpha}_{\rho,l}) \quad (34)$$

where  $r = \sum_{l=1}^{M_T} \tilde{a}_l$ ,  $\tilde{a}_0 = 0$ ,  $\tilde{\alpha}_{\rho,l} = \frac{M_T}{\rho} [(1 + g\rho)^{\tilde{a}_l} - (1 + g\rho)^{\tilde{a}_l - 1}]$ , and  $F_{X_l}(\cdot)$  is given by (33).

As in Section III-A, the lower bound (34) is maximized using nonlinear programming over  $\{\tilde{a}_l\}$  for each  $r$  and  $\rho$ . The feasible set  $\tilde{\mathcal{A}}_r$  for  $\{\tilde{a}_l\}$  is similar to that for  $\{a_l\}$  in Section III-A

$$\tilde{\mathcal{A}}_r = \left\{ (\tilde{a}_1, \tilde{a}_2, \dots, \tilde{a}_{M_T}) \mid \tilde{a}_{l-1} < \tilde{a}_l < \frac{r - \sum_{k=1}^{l-1} \tilde{a}_k}{M_T - l + 1}, \right. \\ \left. l = 1, 2, \dots, M_T - 1; \tilde{a}_{M_T} = r - \sum_{k=1}^{M_T-1} \tilde{a}_k \right\}. \quad (35)$$

**C. Finite-SNR Diversity Gain**

The lower bounds on outage probability given in (17) and (34) can be used to estimate the diversity gain as a function of SNR and multiplexing gain. The result is summarized in the following theorem.

$$F_{X_l}(x) = \begin{cases} \frac{\gamma(M_R - M_T + 2l - 1, (K+1)x)}{\Gamma(M_R - M_T + 2l - 1)}, & l = 1, 2, \dots, M_T - 1 \\ e^{-KM_R M_T} \sum_{n=0}^{\infty} \frac{(KM_R M_T)^n}{n!} \frac{\gamma(M_R + M_T - 1 + n, (K+1)x)}{\Gamma(M_R + M_T - 1 + n)}, & l = M_T. \end{cases} \quad (33)$$

*Theorem 3:* For SNR  $\rho$  and multiplexing gain  $r$ , an estimate of the diversity gain is given by (36) shown at the bottom of the page, where  $(a_1, a_2, \dots, a_{N_T}) \in \mathcal{A}_r$  and  $(\tilde{a}_1, \tilde{a}_2, \dots, \tilde{a}_{M_T}) \in \tilde{\mathcal{A}}_r$  are chosen to maximize the lower bounds (17) and (34), respectively, and  $F'(x) = dF/dx$ .

*Proof:* The proof follows from substituting the lower bounds in (17) and (34) into (5).  $\square$

From the diversity gain (36), the high-SNR asymptotic behavior can be determined, as given in the following.

*Corollary 1:* The high-SNR diversity gain for multiplexing gain  $r$  is

$$\lim_{\rho \rightarrow \infty} \hat{d}(r, \rho) = \begin{cases} \min_{b_l \in \mathcal{B}_r} \sum_{l=1}^{N_T} (M_R - N_T + 2l - 1)b_l, \\ \text{correlated Rayleigh fading} \\ \min_{\tilde{b}_l \in \tilde{\mathcal{B}}_r} \sum_{l=1}^{M_T} (M_R - M_T + 2l - 1)\tilde{b}_l, \\ \text{Rician fading} \end{cases} \quad (37)$$

where  $\mathcal{B}_r = \{(b_1, b_2, \dots, b_{N_T}) \mid 0 \leq b_{N_T} \leq b_{N_T-1} \leq \dots \leq b_1, \sum_{l=1}^{N_T} (1 - b_l)^+ < r\}$ ,  $\tilde{\mathcal{B}}_r = \{(\tilde{b}_1, \tilde{b}_2, \dots, \tilde{b}_{M_T}) \mid 0 \leq \tilde{b}_{M_T} \leq \tilde{b}_{M_T-1} \leq \dots \leq \tilde{b}_1, \sum_{l=1}^{M_T} (1 - \tilde{b}_l)^+ < r\}$ , and  $(x)^+ = \max(0, x)$ .

*Proof:* The proof is given in Appendix IV.  $\square$

From the comparison of (37) with the results in [4], the high-SNR diversity gain is equal to the asymptotic diversity gain  $d_{\text{asymptotic}}$  defined by (3) for both Rayleigh fading with a full-rank transmit covariance matrix ( $N_T = M_T$ ) and Rician fading. Hence, the finite-SNR framework for diversity analysis introduced in this paper can be viewed as a generalization of previous asymptotic analysis in the literature. Furthermore, since spatial correlation and LOS components do not affect the high-SNR diversity gain, the finite-SNR analysis presented here is essential to understanding MIMO system performance in realistic propagation conditions.

#### IV. OUTAGE AND FINITE-SNR DIVERSITY PERFORMANCE: OSTBC

In this section, closed-form expressions for the outage probabilities of OSTBC are computed for both correlated Rayleigh fading and Rician fading. These expressions are used to compute the exact finite-SNR diversity gains of OSTBC. The mutual information (conditioned on the channel realization) for OSTBC with spatial code rate  $r_s$  is given by [15]

$$I_{\text{OSTBC}} = r_s \log_2 \left( 1 + \frac{\rho}{M_T} \|\mathbf{H}\|_F^2 \right). \quad (38)$$

The spatial code rate  $r_s$  is equal to the average number of independent constellation symbols transmitted per channel use through the  $M_T$  transmit antennas. For example,  $r_s = 1$  for the Alamouti space-time code [25], and  $r_s = 1/2$  or  $r_s = 3/4$  for the complex orthogonal designs given in [26]. Since  $\|\mathbf{H}\|_F^2 = \text{tr}(\mathbf{A}_{\text{corr}})$  for correlated Rayleigh fading and  $\|\mathbf{H}\|_F^2 =$

$\text{tr}(\mathbf{A}_{\text{Rice}})$  for Rician fading, the following lemma is needed to determine the outage probability of OSTBC.

*Lemma 4:* The cdfs of  $\|\mathbf{H}\|_F^2$  are given by

$$F_{\text{tr}(\mathbf{A}_{\text{corr}})}(x) = \prod_{n=1}^{N_T} \left( \frac{\mu_1}{\mu_n} \right)^{M_R} \times \sum_{k=0}^{\infty} \frac{\tilde{\delta}_k \gamma(M_R N_T + k, x/\mu_1)}{\Gamma(M_R N_T + k)} \quad \text{correlated Rayleigh fading} \quad (39)$$

$$F_{\text{tr}(\mathbf{A}_{\text{Rice}})}(x) = e^{-KM_R M_T} \sum_{n=0}^{\infty} \frac{(KM_R M_T)^n}{n!} \cdot \frac{\gamma(M_R M_T + n, (K+1)x)}{\Gamma(M_R M_T + n)} \quad \text{Rician fading} \quad (40)$$

where

$$\tilde{\delta}_0 = 1$$

$$\tilde{\delta}_{k+1} = \frac{M_R}{k+1} \sum_{i=1}^{k+1} \left[ \sum_{j=1}^{N_T} \left( 1 - \frac{\mu_1}{\mu_j} \right)^i \right] \tilde{\delta}_{k+1-i} \quad k = 0, 1, \dots \quad (41)$$

*Proof:* The proof is given in Appendix V.  $\square$

The outage probability of OSTBC can now be stated as follows.

*Theorem 4:* For OSTBC, the outage probability is given by

$$P_{\text{out}}^{\text{OSTBC}}(r, \rho) = \begin{cases} F_{\text{tr}(\mathbf{A}_{\text{corr}})}(\check{\alpha}_{\rho, r_s}), & \text{correlated Rayleigh fading} \\ F_{\text{tr}(\mathbf{A}_{\text{Rice}})}(\check{\alpha}_{\rho, r_s}), & \text{Rician fading} \end{cases} \quad (42)$$

where  $\check{\alpha}_{\rho, r_s} = \frac{M_T}{\rho} [(1 + g\rho)^{r/r_s} - 1]$ .

*Proof:* The proof follows from the mutual information expression for OSTBC given by (38). For instance, the outage probability for correlated Rayleigh fading is given by

$$P_{\text{out,corr}}^{\text{OSTBC}}(r, \rho) = \Pr \left[ r_s \log_2 \left( 1 + \frac{\rho}{M_T} \|\mathbf{H}\|_F^2 \right) < r \log_2(1 + g\rho) \right] \quad (43)$$

$$= \Pr \left[ \|\mathbf{H}\|_F^2 < \frac{M_T}{\rho} [(1 + g\rho)^{r/r_s} - 1] \right] \quad (44)$$

$$= F_{\text{tr}(\mathbf{A}_{\text{corr}})}(\check{\alpha}_{\rho, r_s}). \quad (45)$$

$\square$

The diversity gain is then obtained by substituting (45) into (5), and as summarized in the following.

*Theorem 5:* The diversity gain for OSTBC as a function of SNR  $\rho$  and multiplexing  $r$  is given by

$$\hat{d}(r, \rho) = \begin{cases} \sum_{l=1}^{N_T} \frac{F'_{T_l}(\alpha_{\rho, l})}{F_{T_l}(\alpha_{\rho, l})} \left[ \alpha_{\rho, l} - \frac{M_T g}{1+g\rho} (a_l(1+g\rho)^{a_l} - a_{l-1}(1+g\rho)^{a_{l-1}}) \right] & \text{correlated Rayleigh fading} \\ \sum_{l=1}^{M_T} \frac{F'_{X_l}(\check{\alpha}_{\rho, l})}{F_{X_l}(\check{\alpha}_{\rho, l})} \left[ \check{\alpha}_{\rho, l} - \frac{M_T g}{1+g\rho} (\tilde{a}_l(1+g\rho)^{\tilde{a}_l} - \tilde{a}_{l-1}(1+g\rho)^{\tilde{a}_{l-1}}) \right] & \text{Rician fading} \end{cases} \quad (36)$$

$$\mathbf{R}_T = \begin{bmatrix} 1.0000 & 0.0043 + 0.9789i \\ 0.0043 - 0.9789i & 1.0000 \end{bmatrix}, \quad \text{for } M_T = 2 \quad (49)$$

$$\mathbf{R}_T = \begin{bmatrix} 1.0000 & 0.0043 + 0.9789i & -0.9172 + 0.0077i \\ 0.0043 - 0.9789i & 1.0000 & 0.0043 + 0.9789i \\ -0.9172 - 0.0077i & 0.0043 - 0.9789i & 1.0000 \end{bmatrix}, \quad \text{for } M_T = 3 \quad (50)$$

$$\mathbf{R}_T = \begin{bmatrix} 1.0000 & 0.0043 + 0.9789i & -0.9172 + 0.0077i & -0.0092 - 0.8197i \\ 0.0043 - 0.9789i & 1.0000 & 0.0043 + 0.9789i & -0.9172 + 0.0077i \\ -0.9172 - 0.0077i & 0.0043 - 0.9789i & 1.0000 & 0.0043 + 0.9789i \\ -0.0092 + 0.8197i & -0.9172 - 0.0077i & 0.0043 - 0.9789i & 1.0000 \end{bmatrix}, \quad \text{for } M_T = 4. \quad (51)$$

$$d_{\text{OSTBC}}(r, \rho) = \begin{cases} \left[ \check{\alpha}_{\rho, r_s} - \frac{rgM_T}{r_s}(1 + g\rho)^{r/r_s - 1} \right] \cdot \frac{F'_{\text{tr}(\mathbf{A}_{\text{corr}})}(\check{\alpha}_{\rho, r_s})}{F_{\text{tr}(\mathbf{A}_{\text{corr}})}(\check{\alpha}_{\rho, r_s})}, & \text{correlated Rayleigh fading} \\ \left[ \check{\alpha}_{\rho, r_s} - \frac{rgM_T}{r_s}(1 + g\rho)^{r/r_s - 1} \right] \cdot \frac{F'_{\text{tr}(\mathbf{A}_{\text{Rice}})}(\check{\alpha}_{\rho, r_s})}{F_{\text{tr}(\mathbf{A}_{\text{Rice}})}(\check{\alpha}_{\rho, r_s})}, & \text{Rician fading.} \end{cases} \quad (46)$$

The high-SNR diversity gain of OSTBC can be determined from (46), as given in Corollary 2. The proof follows reasoning similar to that of Corollary 1.

*Corollary 2:* The high-SNR diversity gain of OSTBC for multiplexing gain  $r$  is

$$\lim_{\rho \rightarrow \infty} d_{\text{OSTBC}}(r, \rho) = d_0 \left[ 1 - \frac{r}{r_s} \right], \quad 0 \leq r \leq r_s \quad (47)$$

where

$$d_0 = \begin{cases} M_R N_T, & \text{correlated Rayleigh fading} \\ M_R M_T, & \text{Rician fading.} \end{cases} \quad (48)$$

As before for general MIMO systems, the high-SNR asymptotic diversity gain for OSTBC does not depend on spatial correlation or LOS components. Hence, it is necessary to consider finite SNRs for the diversity–multiplexing tradeoff in order to determine the effect of realistic propagation conditions.

### V. NUMERICAL RESULTS

Numerical results are now presented for the finite-SNR outage and diversity analysis given in Sections III and IV. Uniform linear arrays with half-wavelength antenna spacing are assumed at the transmitter and receiver. For correlated Rayleigh fading, a single transmit scattering cluster is assumed with angle of departure of  $30^\circ$  from broadside and a uniform power azimuth spectrum with full-width angle spread of  $15^\circ$ . With these parameters, the transmit covariance matrices for  $M_T = 2, 3, 4$  are given in (49)–(51) at the top of the page. For Rician fading, K-factors of 5 and 10 dB are used. These parameters are similar to those used in the IEEE 802.11 WLAN Task Group N [27].

Fig. 2 is a plot of the outage probability versus SNR for correlated Rayleigh fading with  $M_R = M_T = g = 2$ . The lower

bound (17) is plotted as well as results of Monte Carlo simulations for the exact outage probability. Although there is a gap between the actual outage probability and the lower bound, it can be seen that the *slope* of the lower bound is very similar to that of the actual outage probability curve, in particular at low SNRs. In fact, as shown in Fig. 3, the diversity–multiplexing tradeoff curves obtained from (36) are very close to the simulated curves at SNRs of 5 and 10 dB. Note that (36) is typically larger than the actual diversity gain since  $\hat{d}(r, \rho)$  is derived using the lower bound (17) on outage probability. Nevertheless, the estimate  $\hat{d}(r, \rho)$  agrees with the simulation value as  $r \rightarrow 0$ . From Fig. 3, transmit correlation causes much lower diversity gain at realistic SNRs than the asymptotic result obtained in [4] for  $\text{SNR} \rightarrow \infty$ .

Finite-SNR diversity–multiplexing tradeoff curves based on  $\hat{d}(r, \rho)$  given in (36) are plotted in Fig. 4 for  $M_R = M_T = g = 2$  and several different fading scenarios with  $\text{SNR} = 10$  dB. As expected, the tradeoff curve for correlated Rayleigh fading is greatly below the curve for i.i.d. Rayleigh fading. A qualitatively different behavior is observed for Rician fading. At moderate SNRs and a fixed multiplexing gain  $r$  satisfying  $0 < r_{\min} < r < 1$  for some  $r_{\min}$ , the presence of a LOS component gives rise to a steep drop in outage probability, as seen in Fig. 5. As the SNR increases, the minimum eigenvalue of  $\mathbf{H}^* \mathbf{H}$  begins to affect the outage probability and causes a flatter outage probability curve (lower diversity gain). Hence, for  $0 < r_{\min} < r < 1$ , the log-log plot of outage probability versus SNR (Fig. 5) contains an inflection point, and the diversity gain at moderate SNRs is larger than the high-SNR asymptote. For  $r < r_{\min}$ , the impact of the LOS component on the outage probability slope is less significant since the sensitivity of the rate adaptation algorithm is quite low. Thus, diversity gain is less than the high-SNR asymptote for  $r < r_{\min}$ . From the numerical results, a typical value of  $r_{\min}$  is around 0.25 for  $K = 5$  dB and around 0.1 for  $K = 10$  dB ( $M_R = M_T = g = 2, 3, 4$ ). Also note that all the curves for  $\text{SNR} = 10$  dB converge at  $r = 0$ . Finally, for  $r > 1$ , the diversity gain in Rician fading approaches zero rapidly since the rank-one LOS matrix limits the effective degrees of freedom in the channel. Note that as  $K \rightarrow \infty$ , the Rician fading channel approaches a rank-one AWGN channel such that the outage probability is unity for  $r > 1$  and zero for  $r < 1$ .

From the diversity estimates given in (36) and the exact diversity gain for OSTBC given in (46), three-way tradeoff surfaces of diversity gain, multiplexing gain, and SNR are plotted

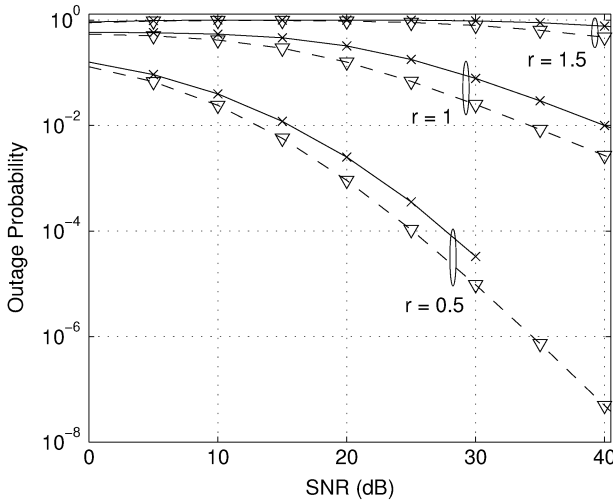


Fig. 2. Outage probability for different multiplexing gains  $r$ ,  $M_R = M_T = g = 2$ , and correlated Rayleigh fading. The solid curves are exact simulation results and the dashed curves are the lower bounds obtained using (17).

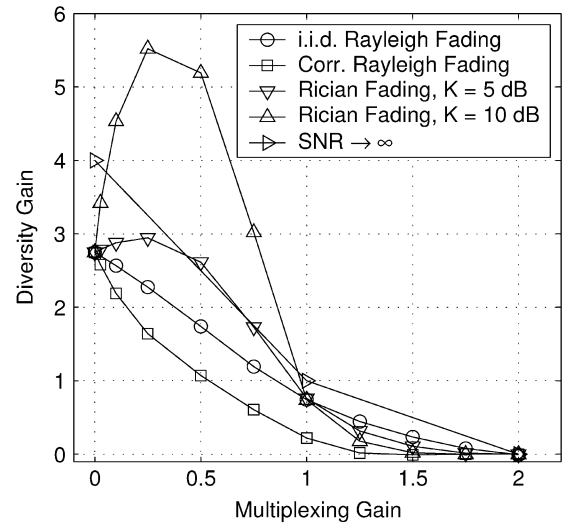


Fig. 4. Finite-SNR diversity-multiplexing tradeoff curves obtained using (36) for  $M_R = M_T = g = 2$  and different fading scenarios with SNR = 10 dB.

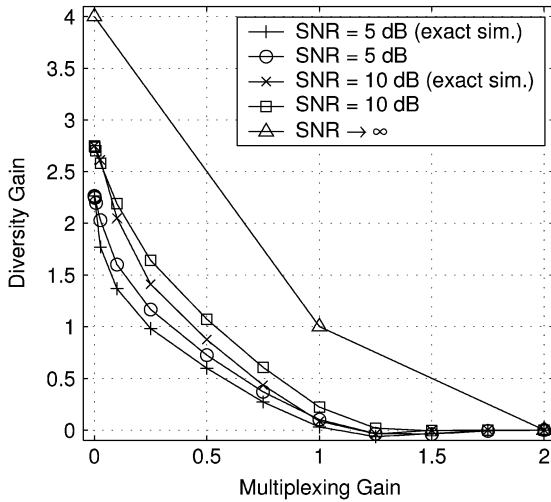


Fig. 3. Diversity gain versus multiplexing gain for  $M_R = M_T = g = 2$  and correlated Rayleigh fading. The actual diversity gain from Monte Carlo simulations is plotted for SNRs of 5 and 10 dB.

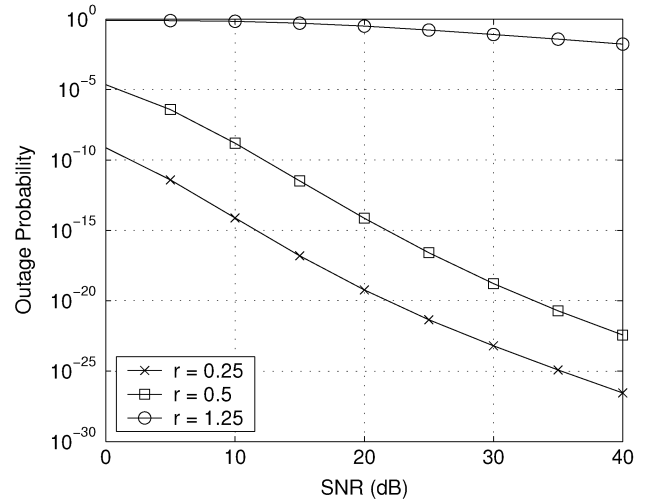


Fig. 5. Outage probability lower bounds (34) for different multiplexing gains  $r$ ,  $M_R = M_T = g = 2$ , and Rician fading with  $K = 10$  dB.

in Figs. 6–8 for 1)  $M_R = M_T = g = 4$  with correlated Rayleigh fading, 2)  $M_R = M_T = g = 4$  with Rician fading ( $K = 5$  dB), and 3)  $M_R = M_T = g = 2$  with the Alamouti space-time code and Rician fading ( $K = 5$  dB). From Fig. 6, spatial correlation significantly reduces the achievable diversity gain and causes slow convergence with SNR of the diversity-multiplexing tradeoff curve to the high-SNR asymptotic result. As was observed in Fig. 4, the increase in diversity gain due to Rician fading at moderate SNRs can be seen in Figs. 7 and 8.

VI. DISCUSSION

The finite-SNR framework for the diversity-multiplexing tradeoff provides useful insight into MIMO performance under realistic propagation conditions. As demonstrated by Corollaries 1 and 2, the effects of spatial correlation and LOS components on the diversity-multiplexing tradeoff cannot be

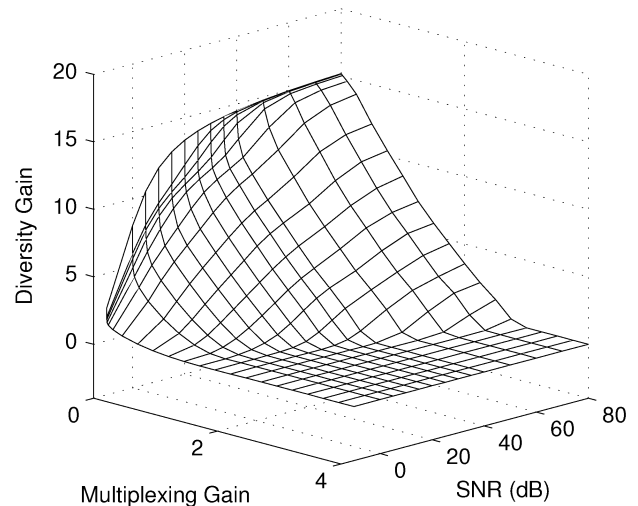


Fig. 6. Diversity gain estimate (36) versus multiplexing gain and SNR for  $M_R = M_T = g = 4$  and correlated Rayleigh fading.

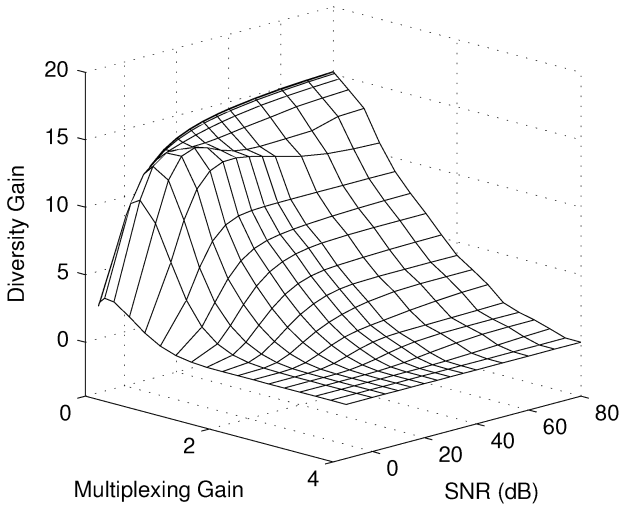


Fig. 7. Diversity gain estimate (36) versus multiplexing gain and SNR for  $M_R = M_T = g = 4$  and Rician fading with  $K = 5$  dB.

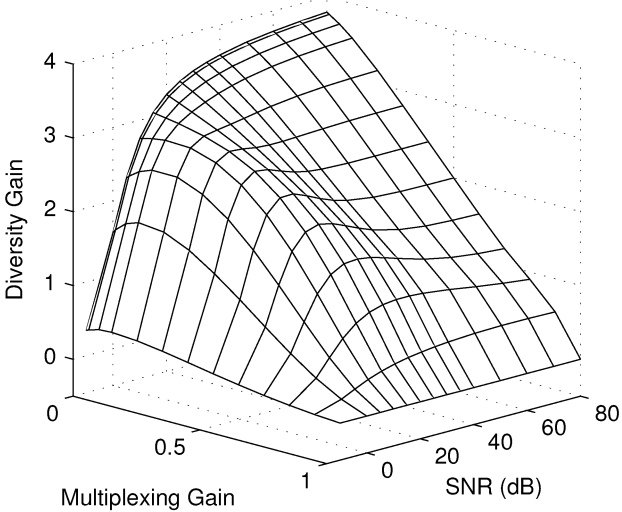


Fig. 8. Diversity gain (46) versus multiplexing gain and SNR for Alamouti code with  $M_R = M_T = g = 2$  and Rician fading ( $K = 5$  dB).

observed at high-SNR. In contrast, the results given in Section V for finite SNR quantify the effect of these propagation conditions on the diversity–multiplexing tradeoff. The reason for the difference can be explained intuitively as follows. As the SNR approaches infinity, only the *number* of channel eigenmodes determines the performance. The *relative strength* of these eigenmodes do not affect high-SNR behavior. Since spatial correlation and LOS components primarily affect the condition number of the channel matrix, the impact of such nonideal propagation effects can be captured only by analyzing the performance at finite SNR. Furthermore, the finite-SNR diversity–multiplexing tradeoff exhibits qualitatively different behavior for Rician channels, as seen in Figs. 4, 7, and 8. From (37) and (47), this behavior is not observed in the limit  $\text{SNR} \rightarrow \infty$  since for finite Rician  $K$ -factors, the overall MIMO channel matrix is still full rank with probability one, although the condition number is increased.

Finite-SNR diversity–multiplexing tradeoff curves are useful to develop a systematic approach for space–time code design for various propagation conditions. In the literature, the impact of channel correlation is often studied for the extremes of high and low SNRs. As aforementioned, nonideal channel conditions do not affect high-SNR performance. In [28], the low-SNR region is studied by assuming a certain fraction  $f$  of the channel eigenvalues are sufficiently small such that they do not contribute to the mutual information (8); the remaining eigenvalues are assumed sufficiently large such that the term “1+” in (8) can be ignored. Based on these assumptions, the pairwise error probability (PEP), diversity gain, and coding gain of a space–time code are approximated. Code design criteria are proposed for correlated channels by taking into account finite SNR. Because the fraction  $f$  is difficult to determine, simulations are used to evaluate the impact of nonideal propagation conditions. In this context, the finite-SNR diversity–multiplexing tradeoff represents a useful analysis tool to evaluate the performance of codes designed according to new criteria such as those given in [28]. The finite-SNR diversity gain for a given multiplexing gain quantifies the strength of the eigenmodes at each SNR without resorting to an ad-hoc determination of the fraction  $f$ . Furthermore, the finite-SNR framework can be used to evaluate the performance of codes that are approximately universal (at high SNR) [29]. Such codes achieve the asymptotic (high-SNR) diversity–multiplexing tradeoff for every slow fading channel. However, different codes will in general have different performance at finite SNR. Detailed performance analysis of space–time codes and new code design criteria based on the finite-SNR diversity–multiplexing tradeoff are interesting topics for future research.

An important property of the finite-SNR diversity gain is the limiting behavior as the multiplexing gain approaches zero. This region is most important for diversity gain since at low multiplexing gains, the rate adaptation strategy is not very sensitive to changes in SNR. In other words, the data rate does not change dramatically with SNR. Such a conservative rate adaptation strategy is usually employed to benefit from increased reliability using spatial diversity. With this motivation, the diversity gain for  $r \rightarrow 0$  is given in the following theorem.

*Theorem 6:* The diversity gain as  $r \rightarrow 0$  of a rate-adaptive MIMO system for SNR  $\rho$  and array gain  $g$  is

$$\lim_{r \rightarrow 0} \hat{d}(r, \rho) = d_0 \left[ 1 - \frac{g\rho}{(1 + g\rho) \ln(1 + g\rho)} \right] \quad (52)$$

where  $d_0$  is given in (48). The result also holds for the case of OSTBC transmission.

*Proof:* The proof is given in Appendix VI.  $\square$

Fig. 9 is a plot of the normalized limiting diversity gain,  $\lim_{r \rightarrow 0} \hat{d}(r, \rho)/d_0$ , as a function of  $\rho$  for  $g = 2, 3, 4$ . From the plot, the diversity gain for SNRs between 3–20 dB is only around 50%–83% of the asymptotic value for practical numbers of antennas. This result indicates that the high-SNR diversity gain of  $d_0$  is often quite optimistic and is close to the actual diversity gain only for SNR greater than 40 dB. The slow convergence of the diversity gain indicates that sacrificing data rate by using a low multiplexing gain does not provide the expected asymptotic diversity gain at realistic SNR. The achievable

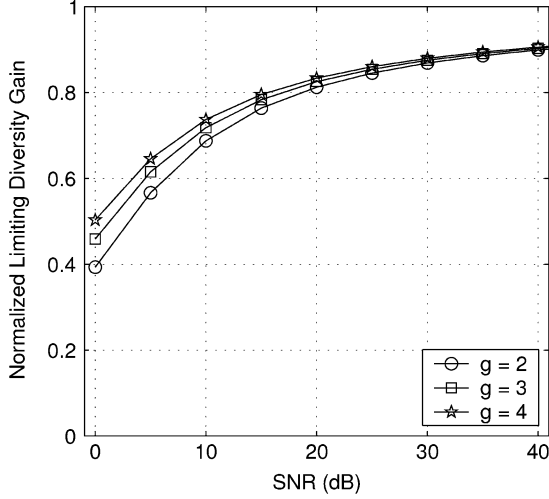


Fig. 9. Normalized limiting diversity gain as a function of SNR.

diversity gain predicted by Theorem 6 and Fig. 9 is useful to determine the actual drop in PER as the SNR increases for a conservative rate adaptation policy ( $r \rightarrow 0$ ). Such insight can be used to select the rate adaptation algorithm at a particular SNR.

Note that the diversity gain as  $r \rightarrow 0$  depends neither on covariance matrix eigenvalues nor on Rician K-factors, as seen in Fig. 4. As  $r \rightarrow 0$ , the spectral efficiency  $R$  approaches zero. As stated in [30], the infinite-bandwidth limit of zero spectral efficiency is not affected by fading. In fact, the limiting diversity gain expression (52) has the following interesting interpretation in terms of the wideband slope [30] and the high-SNR slope [31] of spectral efficiency. Let  $\mathcal{C} = \log_2(1 + g\rho)$  denote the capacity (in bits per second/Hertz) of an AWGN channel with array gain  $g$ , and let  $E_b/N_0$  denote the energy-per-bit normalized to the one-sided noise spectral level. From (52), the normalized limiting diversity gain can be written as follows:

$$\begin{aligned}
 \frac{1}{d_0} \lim_{r \rightarrow 0} \hat{d}(r, \rho) &= 1 - \frac{g\rho}{(1 + g\rho) \ln(1 + g\rho)} \\
 &= 1 - \rho \frac{d \ln \mathcal{C}}{d\rho} \\
 &= 1 - \frac{d \log_2 \mathcal{C}}{d \log_2 \rho} \\
 &= \frac{d \log_2 \left( \frac{\rho}{\mathcal{C}} \right)}{d \log_2 \rho} \\
 &= \frac{d \log_2 \left( \frac{E_b}{N_0} \right)}{d \log_2 \rho} \\
 &= \frac{\frac{d\mathcal{C}}{d \log_2 \rho}}{\frac{d\mathcal{C} \left( \frac{E_b}{N_0} \right)}{d \log_2 \left( \frac{E_b}{N_0} \right)}} \quad (53)
 \end{aligned}$$

where  $E_b/N_0 = \rho/\mathcal{C}$  and  $\mathcal{C}(E_b/N_0)$  is the AWGN channel capacity as a function of  $E_b/N_0$ . From (53), the normalized limiting diversity gain measures the ratio of the slope of capacity versus SNR to the slope of capacity versus  $E_b/N_0$ . In this context, it is insightful to consider the wideband slope and

the high-SNR slope of spectral efficiency, respectively, defined by [30], [31]

$$S_0 = \lim_{\rho \rightarrow 0} \frac{d\mathcal{C} \left( \frac{E_b}{N_0} \right)}{d \log_2 \left( \frac{E_b}{N_0} \right)} \quad (54)$$

$$\begin{aligned}
 S_\infty &= \lim_{\rho \rightarrow \infty} \frac{d\mathcal{C} \left( \frac{E_b}{N_0} \right)}{d \log_2 \left( \frac{E_b}{N_0} \right)} \\
 &= \lim_{\rho \rightarrow \infty} \rho \frac{d\mathcal{C}}{d\rho} \ln 2 \\
 &= \lim_{\rho \rightarrow \infty} \frac{d\mathcal{C}}{d \log_2 \rho}. \quad (55)
 \end{aligned}$$

In AWGN channels,  $S_0 = 2$  and  $S_\infty = 1$ . Furthermore, the following inequalities hold:

$$0 < \frac{d\mathcal{C}}{d \log_2 \rho} < S_\infty < \frac{d\mathcal{C} \left( \frac{E_b}{N_0} \right)}{d \log_2 \left( \frac{E_b}{N_0} \right)} < S_0. \quad (56)$$

At low SNR, the numerator of (53) approaches zero while the denominator approaches  $S_0$ , and, hence, the normalized limiting diversity gain approaches zero. At high SNR, both the numerator and denominator approach  $S_\infty$ , and the normalized limiting diversity gain approaches unity.

Another interesting interpretation of the normalized limiting diversity gain arises from considering the relation between mutual information and minimum mean-square error (MMSE) [32]. Consider a continuous-time Gaussian channel and Gaussian input  $X(t)$  with power spectral density given by

$$S_X(f) = \begin{cases} g, & |f| \leq W \\ 0, & \text{otherwise} \end{cases} \quad (57)$$

where  $g$  is the array gain defined in Section II. The mutual information rate for this channel (in nats/s) is then  $I(\rho) = W \ln(1 + g\rho)$ . Let  $\text{mmse}(\rho)$  and  $\text{cmmse}(\rho)$  denote the noncausal MMSE and causal MMSE, respectively, in estimating the input given the channel output. It is shown in [32] that

$$\text{mmse}(\rho) = 2 \frac{dI(\rho)}{d\rho} \quad (58)$$

$$\text{cmmse}(\rho) = \frac{2I(\rho)}{\rho} \quad (59)$$

Note that (58) and (59) hold under more general conditions. Hence, the normalized limiting diversity gain can be rewritten as follows:

$$\frac{1}{d_0} \lim_{r \rightarrow 0} \hat{d}(r, \rho) = 1 - \frac{\text{mmse}(\rho)}{\text{cmmse}(\rho)}. \quad (60)$$

Thus, the normalized limiting diversity gain can be interpreted as difference between the causal MMSE and the noncausal MMSE relative to the causal MMSE of a continuous-time Gaussian channel. An interesting direction for future research is to explore in greater detail the relations among the finite-SNR diversity-multiplexing tradeoff, spectral efficiency in the wideband and high-SNR regimes, and the link between mutual information and MMSE estimation.

VII. CONCLUSION

Finite SNRs are important in analyzing the diversity–multiplexing tradeoff of MIMO systems in realistic environments. This paper presents a nonasymptotic framework of this tradeoff by introducing finite-SNR definitions of diversity and multiplexing gains. Based on these definitions, diversity gains are computed as functions of the multiplexing gain and SNR for correlated Rayleigh fading and Rician fading. The finite-SNR diversity gain allows accurate estimation of the additional power required to decrease the error probability by a specified value when rate adaptation is employed in the MIMO system. For a general MIMO system, the diversity gain is estimated using lower bounds on the outage probability for a fixed multiplexing gain. The diversity estimate is typically slightly above the exact simulation value. Exact diversity gain expressions are obtained for OSTBC transmission. Spatial correlation significantly lowers the achievable diversity gain at finite SNR. The presence of LOS components in Rician fading yields diversity gains higher than the high-SNR asymptotic values at some SNRs and multiplexing gains; for multiplexing gains larger than unity, the diversity gains are near zero.

As the multiplexing gain approaches zero, the normalized limiting diversity gain as a function of SNR is the same for different MIMO systems and propagation environments. The limiting diversity gain can be interpreted in terms of the wideband slope and the high-SNR slope of spectral efficiency. In addition, the normalized limiting diversity gain is equal to the difference between the causal MMSE and noncausal MMSE relative to the causal MMSE in estimating the input of a continuous-time Gaussian channel given the channel output. The limiting diversity gain is much lower than the high-SNR asymptotic value, a fact that has implications for MIMO systems with conservative rate adaptation strategies. The insights gained from the finite-SNR diversity–multiplexing tradeoff analysis are useful to design MIMO systems for realistic SNRs and propagation environments.

APPENDIX I  
PROOF OF LEMMA 1

Let the eigenvalue decomposition of  $\mathbf{R}_T$  be  $\mathbf{R}_T = \mathbf{U}_T \tilde{\mathbf{D}}_T \mathbf{U}_T^*$ , where  $\mathbf{U}_T$  is a  $M_T \times M_T$  unitary matrix,  $\tilde{\mathbf{D}}_T = \text{blkdiag}(\mathbf{D}_T, \mathbf{0}_{(M_T-N_T) \times (M_T-N_T)})$ , and  $\text{blkdiag}$  denotes block diagonal concatenation. From (7),  $\mathbf{H} = \mathbf{H}_w \mathbf{R}_T^{1/2}$ , and the identity  $\det(\mathbf{I} + \mathbf{A}\mathbf{B}) = \det(\mathbf{I} + \mathbf{B}\mathbf{A})$  [33], the mutual information is given by

$$\begin{aligned} I_{\text{corr}} &= \log_2 \det \left[ \mathbf{I}_{M_R} + \frac{\rho}{M_T} \mathbf{H}_w \mathbf{R}_T \mathbf{H}_w^* \right] \\ &= \log_2 \det \left[ \mathbf{I}_{M_R} + \frac{\rho}{M_T} \mathbf{H}_w \mathbf{U}_T \tilde{\mathbf{D}}_T \mathbf{U}_T^* \mathbf{H}_w^* \right] \\ &\sim \log_2 \det \left[ \mathbf{I}_{M_R} + \frac{\rho}{M_T} \mathbf{H}_w \tilde{\mathbf{D}}_T \mathbf{H}_w^* \right] \end{aligned} \quad (61)$$

where (61) follows from the fact that  $\mathbf{H}_w \mathbf{U}_T \sim \mathbf{H}_w$  since  $\mathbf{U}_T$  is unitary [19]. Now, define the following matrix partition:

$\mathbf{H}_w = [\mathbf{H}_{w,1} \ \mathbf{H}_{w,2}]$ , where  $\mathbf{H}_{w,1}$  is a  $M_R \times N_T$  i.i.d. complex Gaussian matrix. Thus,

$$\begin{aligned} I_{\text{corr}} &\sim \log_2 \det \left[ \mathbf{I}_{M_R} + \frac{\rho}{M_T} \mathbf{H}_{w,1} \mathbf{D}_T \mathbf{H}_{w,1}^* \right] \\ &= \log_2 \det \left[ \mathbf{I}_{N_T} + \frac{\rho}{M_T} \mathbf{D}_T \mathbf{H}_{w,1}^* \mathbf{H}_{w,1} \right] \\ &= \log_2 \det \left[ \mathbf{I}_{N_T} + \frac{\rho}{M_T} \left( \mathbf{D}_T^{1/2} \right)^* \mathbf{H}_{w,1}^* \mathbf{H}_{w,1} \mathbf{D}_T^{1/2} \right] \\ &= \log_2 \det \left[ \mathbf{I}_{N_T} + \frac{\rho}{M_T} \left( \mathbf{H}_{w,1} \mathbf{D}_T^{1/2} \right)^* \left( \mathbf{H}_{w,1} \mathbf{D}_T^{1/2} \right) \right] \\ &= \log_2 \prod_{l=1}^{N_T} \left( 1 + \frac{\rho}{M_T} \lambda_{\text{corr},l} \right) \end{aligned} \quad (62)$$

where (62) follows by letting  $\mathbf{A}_{\text{corr}} = (\mathbf{H}_{w,1} \mathbf{D}_T^{1/2})^* (\mathbf{H}_{w,1} \mathbf{D}_T^{1/2})$ .

APPENDIX II  
PROOF OF LEMMA 2

Consider  $\lambda_{\text{corr},l}$ , the  $l$ th smallest eigenvalue of the Wishart matrix  $\mathbf{A}_{\text{corr}}$  and define the  $l \times N_T$  matrix  $\mathbf{X}^* = [\mathbf{I}_l \ \mathbf{0}_{l \times (N_T-l)}]$ . By definition,  $\mathbf{A}_{\text{corr}}$  is full rank (rank  $N_T$ ). For a  $n \times n$  Hermitian matrix  $\mathbf{B}$ , let  $\lambda_i(\mathbf{B}), i = 1, 2, \dots, n$  denote the eigenvalues sorted in ascending order. By Poincaré’s separation theorem [33]

$$\lambda_i(\mathbf{A}_{\text{corr}}^{-1}) \leq \lambda_i(\mathbf{X}^* \mathbf{A}_{\text{corr}}^{-1} \mathbf{X}) \leq \lambda_{N_T-l+i}(\mathbf{A}_{\text{corr}}^{-1}) \quad i = 1, 2, \dots, l. \quad (63)$$

From the relations  $\lambda_i(\mathbf{A}_{\text{corr}}^{-1}) = 1/\lambda_{N_T-i+1}(\mathbf{A}_{\text{corr}})$  and  $\lambda_i(\mathbf{X}^* \mathbf{A}_{\text{corr}}^{-1} \mathbf{X}) = 1/\lambda_{l-i+1}([\mathbf{X}^* \mathbf{A}_{\text{corr}}^{-1} \mathbf{X}]^{-1})$ , (63) can be rewritten as

$$\begin{aligned} \lambda_{l-i+1}(\mathbf{A}_{\text{corr}}) &\leq \lambda_{l-i+1}([\mathbf{X}^* \mathbf{A}_{\text{corr}}^{-1} \mathbf{X}]^{-1}) \\ &\leq \lambda_{N_T-i+1}(\mathbf{A}_{\text{corr}}), \quad i = 1, 2, \dots, l. \end{aligned} \quad (64)$$

From (64) with  $i = 1$

$$\begin{aligned} \lambda_{\text{corr},l} &= \lambda_l(\mathbf{A}_{\text{corr}}) \\ &\leq \lambda_l([\mathbf{X}^* \mathbf{A}_{\text{corr}}^{-1} \mathbf{X}]^{-1}) \\ &\leq \text{tr}([\mathbf{X}^* \mathbf{A}_{\text{corr}}^{-1} \mathbf{X}]^{-1}) \end{aligned} \quad (65)$$

since  $\lambda_l([\mathbf{X}^* \mathbf{A}_{\text{corr}}^{-1} \mathbf{X}]^{-1})$ , the maximum eigenvalue of the  $l \times l$  matrix  $[\mathbf{X}^* \mathbf{A}_{\text{corr}}^{-1} \mathbf{X}]^{-1}$ , is bounded above by the trace.

The matrix  $[\mathbf{X}^* \mathbf{A}_{\text{corr}}^{-1} \mathbf{X}]^{-1}$  can be computed from the following partitions of  $\mathbf{A}_{\text{corr}}$ :

$$\begin{aligned} \mathbf{A}_{\text{corr}} &= \begin{bmatrix} \mathbf{A}_{11,l \times l} & \mathbf{A}_{12,l \times (N_T-l)} \\ \mathbf{A}_{21,(N_T-l) \times l} & \mathbf{A}_{22,(N_T-l) \times (N_T-l)} \end{bmatrix} \\ &= \begin{bmatrix} \mathbf{B}_{11,(l-1) \times (l-1)} & \mathbf{B}_{12,(l-1) \times (N_T-l+1)} \\ \mathbf{B}_{21,(N_T-l+1) \times (l-1)} & \mathbf{B}_{22,(N_T-l+1) \times (N_T-l+1)} \end{bmatrix}. \end{aligned} \quad (66)$$

(67)

$$\mathbf{A}_{11:2}^{-1} = \begin{bmatrix} \mathbf{B}_{11:2}^{-1} & \mathbf{v} \\ \mathbf{v}^* & u \end{bmatrix} \quad (70)$$

$$\mathbf{A}_{11:2} = \begin{bmatrix} \mathbf{B}_{11:2} + \mathbf{B}_{11:2}\mathbf{v}(u - \mathbf{v}^*\mathbf{B}_{11:2}\mathbf{v})^{-1}\mathbf{v}^*\mathbf{B}_{11:2} & -\mathbf{B}_{11:2}\mathbf{v}(u - \mathbf{v}^*\mathbf{B}_{11:2}\mathbf{v})^{-1} \\ -(u - \mathbf{v}^*\mathbf{B}_{11:2}\mathbf{v})^{-1}\mathbf{v}^*\mathbf{B}_{11:2} & (u - \mathbf{v}^*\mathbf{B}_{11:2}\mathbf{v})^{-1} \end{bmatrix}. \quad (71)$$

From (69)

$$[\mathbf{X}^* \mathbf{A}_{\text{corr}}^{-1} \mathbf{X}]^{-1} = \mathbf{A}_{11} - \mathbf{A}_{12} \mathbf{A}_{22}^{-1} \mathbf{A}_{21} \quad (68)$$

$$\equiv \mathbf{A}_{11:2} \quad (69)$$

where  $\mathbf{A}_{11:2}$  is the Schur complement of  $\mathbf{A}_{22}$  in  $\mathbf{A}_{\text{corr}}$ . Similarly, define  $\mathbf{B}_{11:2} = \mathbf{B}_{11} - \mathbf{B}_{12} \mathbf{B}_{22}^{-1} \mathbf{B}_{21}$ . From [19, Th. 3.2.10],  $\mathbf{A}_{11:2} \sim \mathcal{W}_l(M_R - N_T + l, \text{diag}(\mu_1, \mu_2, \dots, \mu_l))$  and  $\mathbf{B}_{11:2} \sim \mathcal{W}_{l-1}(M_R - N_T + l - 1, \text{diag}(\mu_1, \mu_2, \dots, \mu_{l-1}))$ . From the inverse of partitioned matrices, one can show (70) and (71) given at the top of the page, where  $\mathbf{v}$  is a  $(l-1) \times 1$  vector and  $u$  is a scalar. If

$$T_l = \text{tr}(\mathbf{B}_{11:2}\mathbf{v}(u - \mathbf{v}^*\mathbf{B}_{11:2}\mathbf{v})^{-1}\mathbf{v}^*\mathbf{B}_{11:2}) + (u - \mathbf{v}^*\mathbf{B}_{11:2}\mathbf{v})^{-1} \quad (72)$$

then

$$\text{tr}(\mathbf{A}_{11:2}) = \text{tr}(\mathbf{B}_{11:2}) + T_l \quad (73)$$

where  $T_l$  is independent of  $\text{tr}(\mathbf{B}_{11:2})$  [19]. By applying (73) to  $\mathbf{B}_{11:2}$  and to successively smaller upper left submatrices of  $\mathbf{A}_{\text{corr}}$ , it can be seen that

$$\text{tr}(\mathbf{A}_{11:2}) = \sum_{n=1}^l T_n \quad (74)$$

where the  $T_n$  are independent. It remains to determine the distribution of  $T_l, l = 1, 2, \dots, N_T$ . Since  $\mathbf{A}_{11:2}$  and  $\mathbf{B}_{11:2}$  are Wishart matrices, the Laplace transforms of the probability density functions (pdfs) of  $\text{tr}(\mathbf{A}_{11:2})$  and  $\text{tr}(\mathbf{B}_{11:2})$  are given by

$$\mathcal{L}_{\text{tr}(\mathbf{A}_{11:2})}(s) = \frac{1}{\prod_{n=1}^l (1 + s\mu_n)^{M_R - N_T + l}} \quad (75)$$

$$\mathcal{L}_{\text{tr}(\mathbf{B}_{11:2})}(s) = \frac{1}{\prod_{n=1}^{l-1} (1 + s\mu_n)^{M_R - N_T + l - 1}}. \quad (76)$$

From (73) and the independence of  $T_l$  and  $\mathbf{B}_{11:2}$ , the Laplace transform of the pdf of  $T_l$  is

$$\begin{aligned} \mathcal{L}_{T_l}(s) &= \frac{\mathcal{L}_{\text{tr}(\mathbf{A}_{11:2})}(s)}{\mathcal{L}_{\text{tr}(\mathbf{B}_{11:2})}(s)} \\ &= \frac{\prod_{n=1}^{l-1} (1 + s\mu_n)^{M_R - N_T + l - 1}}{\prod_{n=1}^l (1 + s\mu_n)^{M_R - N_T + l}} \\ &= \frac{1}{\left[ \prod_{n=1}^{l-1} (1 + s\mu_n) \right] (1 + s\mu_l)^{M_R - N_T + l}}. \end{aligned} \quad (77)$$

By inspection of (77),  $T_l$  can be written as the sum of independent gamma variables, as given in (11). From (65), (69), and (74),

$$\lambda_{\text{corr},l} \leq \sum_{n=1}^l T_n, \quad l = 1, 2, \dots, N_T. \quad (78)$$

and, hence,

$$\begin{aligned} \Pr[\lambda_{\text{corr},l} < x_l, l = 1, 2, \dots, N_T] \\ \geq \Pr\left[ \sum_{n=1}^l T_n < x_l, l = 1, 2, \dots, N_T \right] \end{aligned} \quad (79)$$

where  $0 < x_1 < x_2 < \dots < x_{N_T}$ .

### APPENDIX III PROOF OF LEMMA 3

The proof is divided into two parts. First, suppose  $l \leq M_T - 1$  and consider the following partitions of  $\mathbf{A}_{\text{Rice}}$ :

$$\mathbf{A}_{\text{Rice}} = \begin{bmatrix} \tilde{\mathbf{A}}_{11,l \times l} & \tilde{\mathbf{A}}_{12,l \times (M_T - l)} \\ \tilde{\mathbf{A}}_{21,(M_T - l) \times l} & \tilde{\mathbf{A}}_{22,(M_T - l) \times (M_T - l)} \end{bmatrix} \quad (80)$$

$$= \begin{bmatrix} \tilde{\mathbf{B}}_{11,(l-1) \times (l-1)} & \tilde{\mathbf{B}}_{12,(l-1) \times (M_T - l + 1)} \\ \tilde{\mathbf{B}}_{21,(M_T - l + 1) \times (l-1)} & \tilde{\mathbf{B}}_{22,(M_T - l + 1) \times (M_T - l + 1)} \end{bmatrix}. \quad (81)$$

As in (69), let  $\tilde{\mathbf{A}}_{11:2} = \tilde{\mathbf{A}}_{11} - \tilde{\mathbf{A}}_{12} \tilde{\mathbf{A}}_{22}^{-1} \tilde{\mathbf{A}}_{21}$  be the Schur complement of  $\tilde{\mathbf{A}}_{22}$  in  $\mathbf{A}_{\text{Rice}}$ . It can be deduced from Problem 10.11 of [19] that  $\tilde{\mathbf{A}}_{11:2} \sim \mathcal{W}_l(M_R - M_T + l, \frac{1}{K+1} \mathbf{I}_l)$  and  $\tilde{\mathbf{B}}_{11:2} \sim \mathcal{W}_{l-1}(M_R - M_T + l - 1, \frac{1}{K+1} \mathbf{I}_{l-1})$  are central Wishart matrices. Proceeding as in Appendix II, one obtains

$$\text{tr}(\tilde{\mathbf{A}}_{11:2}) = \text{tr}(\tilde{\mathbf{B}}_{11:2}) + X_l \quad (82)$$

where the random variable  $X_l$  is independent of  $\text{tr}(\tilde{\mathbf{B}}_{11:2})$ . Thus,

$$\text{tr}(\tilde{\mathbf{A}}_{11:2}) = \sum_{n=1}^l X_n \quad (83)$$

where  $X_n$  are independent. Since the Laplace transforms of the pdfs of  $\text{tr}(\tilde{\mathbf{A}}_{11:2})$  and  $\text{tr}(\tilde{\mathbf{B}}_{11:2})$  for  $l \leq M_T - 1$  are

$$\mathcal{L}_{\text{tr}(\tilde{\mathbf{A}}_{11:2})}(s) = \frac{1}{\left(1 + \frac{s}{K+1}\right)^{l(M_R - M_T + l)}} \quad (84)$$

$$\mathcal{L}_{\text{tr}(\tilde{\mathbf{B}}_{11:2})}(s) = \frac{1}{\left(1 + \frac{s}{K+1}\right)^{(l-1)(M_R - M_T + l - 1)}}, \quad (85)$$

the Laplace transform of the pdf of  $X_l$  is

$$\begin{aligned} \mathcal{L}_{X_l}(s) &= \frac{\mathcal{L}_{\text{tr}(\tilde{\mathbf{A}}_{11:2})}(s)}{\mathcal{L}_{\text{tr}(\tilde{\mathbf{B}}_{11:2})}(s)} \\ &= \frac{1}{\left(1 + \frac{s}{K+1}\right)^{M_R - M_T + 2l - 1}}. \end{aligned} \quad (86)$$

Thus,  $X_l, l = 1, 2, \dots, M_T - 1$  are gamma variables with parameters  $(M_R - M_T + 2l - 1, 1/(K + 1))$ .

Now, suppose  $l = M_T$ . From the partitioned matrix given in (81), the  $(M_T - 1) \times (M_T - 1)$  Schur complement  $\tilde{\mathbf{B}}_{11.2}$  has the central Wishart distribution  $\tilde{\mathbf{B}}_{11.2} \sim \mathcal{W}_{M_T-1}(M_R - 1, \frac{1}{K+1}\mathbf{I}_{M_T-1})$ . In this case

$$\text{tr}(\mathbf{A}_{\text{Rice}}) = \text{tr}(\tilde{\mathbf{B}}_{11.2}) + X_{M_T} \quad (87)$$

where  $X_{M_T}$  is independent of  $\text{tr}(\tilde{\mathbf{B}}_{11.2})$  [19]. From the properties of noncentral Wishart matrices, it can be shown that the Laplace transform of the pdf of  $\text{tr}(\mathbf{A}_{\text{Rice}})$  is given by

$$\mathcal{L}_{\text{tr}(\mathbf{A}_{\text{Rice}})}(s) = \frac{\exp\left[-\frac{KM_R M_T \frac{s}{K+1}}{1 + \frac{s}{K+1}}\right]}{\left(1 + \frac{s}{K+1}\right)^{M_R M_T}}. \quad (88)$$

Thus, the Laplace transform of the pdf of  $X_{M_T}$  is

$$\begin{aligned} \mathcal{L}_{X_{M_T}}(s) &= \frac{\mathcal{L}_{\text{tr}(\mathbf{A}_{\text{Rice}})}(s)}{\mathcal{L}_{\text{tr}(\tilde{\mathbf{B}}_{11.2})}(s)} \\ &= \frac{\exp\left[-\frac{KM_R M_T \frac{s}{K+1}}{1 + \frac{s}{K+1}}\right]}{\left(1 + \frac{s}{K+1}\right)^{M_R + M_T - 1}}. \end{aligned} \quad (89)$$

From (89) and [34],  $X_{M_T}$  is a noncentral gamma random variable with shape parameter  $M_R + M_T - 1$ , noncentrality parameter  $KM_R M_T$ , and scale parameter  $1/(K+1)$ . The cdf of  $X_{M_T}$  is given by (33) with  $l = M_T$ . Thus, similar to (78)

$$\lambda_{\text{Rice},l} \leq \sum_{n=1}^l X_n, \quad l = 1, 2, \dots, M_T \quad (90)$$

and, hence

$$\begin{aligned} \Pr[\lambda_{\text{Rice},l} < x_l, l = 1, 2, \dots, M_T] \\ \geq \Pr\left[\sum_{n=1}^l X_n < x_l, l = 1, 2, \dots, M_T\right] \end{aligned} \quad (91)$$

where  $0 < x_1 < x_2 < \dots < x_{M_T}$ .

#### APPENDIX IV PROOF OF COROLLARY 1

First, consider the case of correlated Rayleigh fading. Since  $a_l > a_{l-1}, l = 1, 2, \dots, N_T$ , we have  $\alpha_{\rho,l} \rightarrow M_T g^{a_l} / \rho^{1-a_l}$  as  $\rho \rightarrow \infty$ . Furthermore, if  $a_l > 1$ ,  $F'_{T_l}(\alpha_{\rho,l}) \rightarrow 0$  as  $\rho \rightarrow \infty$ . Thus, it suffices to consider the case  $a_l \leq 1$ . In this case

$$\begin{aligned} \lim_{\rho \rightarrow \infty} \left[ \alpha_{\rho,l} - \frac{M_T g}{1 + g\rho} (a_l(1 + g\rho)^{a_l} - a_{l-1}(1 + g\rho)^{a_{l-1}}) \right] \\ = \lim_{\rho \rightarrow \infty} \left[ \frac{M_T g^{a_l}}{\rho^{1-a_l}} - \frac{M_T a_l g^{a_l}}{\rho^{1-a_l}} \right] \\ = \lim_{\rho \rightarrow \infty} \frac{M_T g^{a_l}}{\rho^{1-a_l}} (1 - a_l). \end{aligned} \quad (92)$$

In addition

$$\begin{aligned} \lim_{\rho \rightarrow \infty} \frac{F'_{T_l}(\alpha_{\rho,l})}{F_{T_l}(\alpha_{\rho,l})} \\ = \lim_{\rho \rightarrow \infty} \frac{\sum_{k=0}^{\infty} \frac{\delta_{k,l} e^{-\alpha_{\rho,l}/\mu_1} (\alpha_{\rho,l}/\mu_1)^{M_R - N_T + 2l - 2 + k} \frac{1}{\mu_1}}{\Gamma(M_R - N_T + 2l - 1 + k)}}{\sum_{k=0}^{\infty} \frac{\delta_{k,l} \gamma(M_R - N_T + 2l - 1 + k, \alpha_{\rho,l}/\mu_1)}{\Gamma(M_R - N_T + 2l - 1 + k)}} \\ = \lim_{\rho \rightarrow \infty} \frac{(\alpha_{\rho,l}/\mu_1)^{M_R - N_T + 2l - 2} \frac{1}{\mu_1}}{\frac{(\alpha_{\rho,l}/\mu_1)^{M_R - N_T + 2l - 1}}{M_R - N_T + 2l - 1}} \\ = \lim_{\rho \rightarrow \infty} \frac{M_R - N_T + 2l - 1}{\alpha_{\rho,l}} \\ = \lim_{\rho \rightarrow \infty} \frac{(M_R - N_T + 2l - 1)\rho^{1-a_l}}{M_T g^{a_l}} \end{aligned} \quad (93)$$

since  $\gamma(m, x) \approx x^m/m$ ,  $x \ll 1$  and  $\alpha_{\rho,l} \rightarrow 0$  as  $\rho \rightarrow \infty$  for  $a_l \leq 1$ . From (36), (92), and (93),

$$\begin{aligned} \lim_{\rho \rightarrow \infty} \hat{d}(r, \rho) \\ = \lim_{\rho \rightarrow \infty} \sum_{\substack{l=1 \\ a_l \leq 1}}^{N_T} \frac{(M_R - N_T + 2l - 1)\rho^{1-a_l}}{M_T g^{a_l}} \frac{M_T g^{a_l}}{\rho^{1-a_l}} (1 - a_l) \\ = \sum_{l=1}^{N_T} (M_R - N_T + 2l - 1) b_l \end{aligned} \quad (94)$$

where  $b_l = (1 - a_l)^+$ . Note that

$$\begin{aligned} r &= \sum_{l=1}^{N_T} a_l \\ &= \sum_{\substack{l=1 \\ a_l \leq 1}}^{N_T} (1 - b_l)^+ + \sum_{\substack{l=1 \\ a_l > 1}}^{N_T} a_l \\ &> \sum_{l=1}^{N_T} (1 - b_l)^+ \end{aligned} \quad (95)$$

since if  $a_l > 1$   $(1 - b_l)^+ = 1$ . Now, as  $\rho \rightarrow \infty$ , maximizing the lower bound (17) on the outage probability is equivalent to minimizing (94) with respect to  $\{b_l\}$ . From the feasible set  $\mathcal{A}_r$  for  $\{a_l\}$  and (95), the feasible set for  $\{b_l\}$  is  $\mathcal{B}_r = \{(b_1, b_2, \dots, b_{N_T}) \mid 0 \leq b_{N_T} \leq b_{N_T-1} \leq \dots \leq b_1, \sum_{l=1}^{N_T} (1 - b_l)^+ < r\}$ . Thus, the high-SNR diversity gain for correlated Rayleigh fading is

$$\lim_{\rho \rightarrow \infty} \hat{d}(r, \rho) = \min_{b_l \in \mathcal{B}_r} \sum_{l=1}^{N_T} (M_R - N_T + 2l - 1) b_l. \quad (96)$$

For Rician fading, since  $\tilde{a}_l > \tilde{a}_{l-1}, l = 1, 2, \dots, M_T$ ,  $\tilde{\alpha}_{\rho,l} \rightarrow M_T g^{\tilde{a}_l} / \rho^{1-\tilde{a}_l}$  as  $\rho \rightarrow \infty$ . Furthermore, if  $\tilde{a}_l > 1$ ,  $F'_{X_l}(\tilde{\alpha}_{\rho,l}) \rightarrow 0$  as  $\rho \rightarrow \infty$ . From (33), it can be shown in a manner similar to (92) and (93) that for  $\tilde{a}_l \leq 1$ ,

$$\begin{aligned} \lim_{\rho \rightarrow \infty} \left[ \tilde{\alpha}_{\rho,l} - \frac{M_T g}{1 + g\rho} (\tilde{a}_l(1 + g\rho)^{\tilde{a}_l} - \tilde{a}_{l-1}(1 + g\rho)^{\tilde{a}_{l-1}}) \right] \\ = \lim_{\rho \rightarrow \infty} \frac{M_T g^{\tilde{a}_l}}{\rho^{1-\tilde{a}_l}} (1 - \tilde{a}_l). \end{aligned} \quad (97)$$

$$\begin{aligned} & \lim_{\rho \rightarrow \infty} \frac{F'_{X_l}(\tilde{\alpha}_{\rho,l})}{F_{X_l}(\tilde{\alpha}_{\rho,l})} \\ &= \lim_{\rho \rightarrow \infty} \frac{(M_R - M_T + 2l - 1)\rho^{1-\tilde{a}_l}}{M_T g^{\tilde{a}_l}} \end{aligned} \quad (98)$$

Thus, from (36), (97), and (98)

$$\begin{aligned} & \lim_{\rho \rightarrow \infty} \hat{d}(r, \rho) \\ &= \lim_{\rho \rightarrow \infty} \sum_{\substack{l=1 \\ \tilde{a}_l \leq 1}}^{M_T} \frac{(M_R - M_T + 2l - 1)\rho^{1-\tilde{a}_l}}{M_T g^{\tilde{a}_l}} \\ & \quad \cdot \frac{M_T g^{\tilde{a}_l}}{\rho^{1-\tilde{a}_l}} (1 - \tilde{a}_l) \\ &= \sum_{l=1}^{M_T} (M_R - M_T + 2l - 1) \tilde{b}_l \end{aligned} \quad (99)$$

where  $\tilde{b}_l = (1 - \tilde{a}_l)^+$ . Similar to (95),  $r > \sum_{l=1}^{M_T} (1 - \tilde{b}_l)^+$ . Maximizing the lower bound (34) on the outage probability is equivalent to minimizing (99) with respect to  $\{\tilde{b}_l\}$  as  $\rho \rightarrow \infty$ . The feasible set for  $\{\tilde{b}_l\}$  is  $\tilde{\mathcal{B}}_r = \{(\tilde{b}_1, \tilde{b}_2, \dots, \tilde{b}_{N_T}) \mid 0 \leq \tilde{b}_{N_T} \leq \tilde{b}_{N_T-1} \leq \dots \leq \tilde{b}_1, \sum_{l=1}^{M_T} (1 - \tilde{b}_l)^+ < r\}$ . Thus, the high-SNR diversity gain for Rician fading is

$$\lim_{\rho \rightarrow \infty} \hat{d}(r, \rho) = \min_{\tilde{b}_l \in \tilde{\mathcal{B}}_r} \sum_{l=1}^{M_T} (M_R - M_T + 2l - 1) \tilde{b}_l. \quad (100)$$

#### APPENDIX V PROOF OF LEMMA 4

For correlated Rayleigh fading,  $\mathbf{A}_{\text{corr}} = \mathbf{A}_{11 \cdot 2}$ , where  $\mathbf{A}_{11 \cdot 2}$  is the Schur complement defined in (69) with  $l = N_T$ . From (76), the Laplace transform of the pdf of  $\text{tr}(\mathbf{A}_{\text{corr}})$  is

$$\mathcal{L}_{\text{tr}(\mathbf{A}_{\text{corr}})}(s) = \frac{1}{\prod_{n=1}^{N_T} (1 + s\mu_n)^{M_R}}. \quad (101)$$

Thus, from [21], [22], the cdf of  $\text{tr}(\mathbf{A}_{\text{corr}})$  can be written as

$$\begin{aligned} & F_{\text{tr}(\mathbf{A}_{\text{corr}})}(x) \\ &= \prod_{n=1}^{N_T} \left( \frac{\mu_1}{\mu_n} \right)^{M_R} \sum_{k=0}^{\infty} \frac{\tilde{\delta}_k \gamma(M_R N_T + k, x/\mu_1)}{\Gamma(M_R N_T + k)} \end{aligned} \quad (102)$$

where the  $\tilde{\delta}_k$  are defined in (41).

For Rician fading, the Laplace transform of the pdf of  $\text{tr}(\mathbf{A}_{\text{Rice}})$  is given in (88). Thus, from [34],  $\text{tr}(\mathbf{A}_{\text{Rice}})$  is a noncentral gamma random variable with shape parameter  $M_R M_T$ , noncentrality parameter  $K M_R M_T$ , and scale parameter  $1/(K + 1)$ . The cdf of  $\text{tr}(\mathbf{A}_{\text{Rice}})$  is given by (40).

#### APPENDIX VI PROOF OF THEOREM 6

Note that as  $r \rightarrow 0$ ,  $a_l \rightarrow 0$  and  $\tilde{a}_l \rightarrow 0$ , for correlated Rayleigh fading and Rician fading, respectively. Since  $a_l$  and  $\tilde{a}_l$  are functions of  $r$ , the following expansion can be written:

$$a_l = c_l r + o(r), \quad l = 1, 2, \dots, N_T \quad (103)$$

$$\tilde{a}_l = \tilde{c}_l r + o(r), \quad l = 1, 2, \dots, M_T \quad (104)$$

where  $c_l$  and  $\tilde{c}_l$  are the coefficients of expansion. Similarly

$$\alpha_{\rho,l} = \frac{M_T}{\rho} r (c_l - c_{l-1}) \ln(1 + g\rho) + o(r) \quad (105)$$

$$\tilde{\alpha}_{\rho,l} = \frac{M_T}{\rho} r (\tilde{c}_l - \tilde{c}_{l-1}) \ln(1 + g\rho) + o(r). \quad (106)$$

Thus, for correlated Rayleigh fading

$$\begin{aligned} \lim_{r \rightarrow 0} \hat{d}(r, \rho) &= \lim_{r \rightarrow 0} \sum_{l=1}^{N_T} \frac{M_R - N_T + 2l - 1}{\frac{M_T}{\rho} r (c_l - c_{l-1}) \ln(1 + g\rho)} \\ & \quad \cdot \left[ \frac{M_T}{\rho} r (c_l - c_{l-1}) \ln(1 + g\rho) \right. \\ & \quad \left. - \frac{M_T g}{1 + g\rho} (c_l - c_{l-1}) r \right] \\ &= \lim_{r \rightarrow 0} \sum_{l=1}^{N_T} (M_R - N_T + 2l - 1) \\ & \quad \cdot \left[ 1 - \frac{g\rho}{(1 + g\rho) \ln(1 + g\rho)} \right] \\ &= M_R N_T \left[ 1 - \frac{g\rho}{(1 + g\rho) \ln(1 + g\rho)} \right] \end{aligned} \quad (107)$$

since  $\alpha_{\rho,l} \rightarrow 0$  as  $r \rightarrow 0$  implies

$\lim_{r \rightarrow 0} F'_{T_l}(\alpha_{\rho,l})/F_{T_l}(\alpha_{\rho,l}) = \lim_{r \rightarrow 0} [(M_R - N_T + 2l - 1)/\alpha_{\rho,l}]$  using an analysis similar to (93). For Rician fading, the same procedure is used to give the result

$$\lim_{r \rightarrow 0} \hat{d}(r, \rho) = M_R M_T \left[ 1 - \frac{g\rho}{(1 + g\rho) \ln(1 + g\rho)} \right]. \quad (108)$$

Finally, for OSTBC, note that  $\check{\alpha}_{\rho,r_s} = \frac{M_T r}{\rho r_s} \ln(1 + g\rho) + o(r)$ . Furthermore, one can show that

$$\begin{aligned} \lim_{r \rightarrow 0} \frac{F'_{\text{tr}(\mathbf{A}_{\text{corr}})}(\check{\alpha}_{\rho,r_s})}{F_{\text{tr}(\mathbf{A}_{\text{corr}})}(\check{\alpha}_{\rho,r_s})} &= \lim_{r \rightarrow 0} \frac{M_R N_T}{\check{\alpha}_{\rho,r_s}} \\ \lim_{r \rightarrow 0} \frac{F'_{\text{tr}(\mathbf{A}_{\text{Rice}})}(\check{\alpha}_{\rho,r_s})}{F_{\text{tr}(\mathbf{A}_{\text{Rice}})}(\check{\alpha}_{\rho,r_s})} &= \lim_{r \rightarrow 0} \frac{M_R M_T}{\check{\alpha}_{\rho,r_s}}. \end{aligned} \quad (109)$$

Thus

$$\begin{aligned} & \lim_{r \rightarrow 0} d_{\text{OSTBC}}(r, \rho) \\ &= \lim_{r \rightarrow 0} \left[ \frac{M_T r}{\rho r_s} \ln(1 + g\rho) - \frac{r g M_T}{r_s (1 + g\rho)} \right] \frac{d_0}{\frac{M_T r}{\rho r_s} \ln(1 + g\rho)} \\ &= d_0 \left[ 1 - \frac{g\rho}{(1 + g\rho) \ln(1 + g\rho)} \right]. \end{aligned} \quad (110)$$

#### REFERENCES

- [1] V. Tarokh, N. Seshadri, and A. R. Calderbank, "Space-time codes for high data rate wireless communication: Performance criterion and code construction," *IEEE Trans. Inf. Theory*, vol. 44, pp. 744–765, Mar. 1998.
- [2] A. Paulraj and T. Kailath, "Increasing Capacity in Wireless Broadcast Systems Using Distributed Transmission/Directional Reception (DTDR)," U.S. Pat. 5 345 599, 1993.
- [3] P. W. Wolniansky, G. J. Foschini, G. D. Golden, and R. A. Valenzuela, "V-BLAST: An architecture for realizing very high data rates over the rich-scattering wireless channel," in *Proc. URSI ISSSE-98*, Pisa, Italy, Sep. 1998, pp. 295–300.
- [4] L. Zheng and D. N. C. Tse, "Diversity and multiplexing: A fundamental tradeoff in multiple antenna channels," *IEEE Trans. Inf. Theory*, vol. 49, pp. 1073–1096, May 2003.
- [5] *IEEE 802.11: Wireless LAN Medium Access Control (MAC) and Physical Layer (PHY) Specifications: High-Speed Physical Layer in the 5 GHz Band, Supplement to IEEE 802.11 Standard*, 802.11, Sep. 1999.
- [6] H. El Gamal, "On the robustness of space-time coding," *IEEE Trans. Signal Process.*, vol. 50, pp. 2417–2428, Oct. 2002.

- [7] S. Siwamogsatham and M. P. Fitz, "Robust space-time codes for correlated Rayleigh fading channels," *IEEE Trans. Signal Process.*, vol. 50, pp. 2408–2416, Oct. 2002.
- [8] B. Clerckx, L. Vandendriessche, D. Vanhoenacker-Janvier, and A. J. Paulraj, "On the "high SNR" assumption in space-time codes designs," in *Proc. IEEE ICC 2004*, Paris, France, Jun. 2004.
- [9] M. Vajapeyam, J. Geng, and U. Mitra, "Low SNR design of space-time block codes based on union bound and indecomposable error patterns," in *Proc. IEEE ICC 2004*, Paris, France, Jun. 2004.
- [10] C. Berrou and A. Glavieux, "Near optimum error correcting coding and decoding: Turbo-codes," *IEEE Trans. Commun.*, vol. 44, no. 10, pp. 1261–1271, Oct. 1996.
- [11] R. G. Gallager, "Low density parity check codes," *IRE Trans. Inf. Theory*, vol. 8, pp. 21–28, Jan. 1962.
- [12] D. J. C. MacKay, "Good error-correcting codes based on very sparse matrices," *IEEE Trans. Inf. Theory*, vol. 45, no. 2, pp. 399–431, Mar. 1999.
- [13] Z. Wang and G. B. Giannakis, "Outage mutual information of space-time MIMO channels," *IEEE Trans. Inf. Theory*, vol. 50, no. 4, pp. 657–662, Apr. 2004.
- [14] M. Chiani, M. Z. Win, and A. Zanella, "On the capacity of spatially correlated MIMO Rayleigh-fading channels," *IEEE Trans. Inf. Theory*, vol. 49, no. 10, pp. 2363–2371, Oct. 2003.
- [15] A. Paulraj, R. Nabar, and D. Gore, *Introduction to Space-Time Wireless Communications*. Cambridge, U.K.: Cambridge Univ. Press, 2003.
- [16] E. Telatar, "Capacity of multi-antenna Gaussian channels," *European Trans. Telecomm. (ETT)*, vol. 10, no. 6, pp. 585–596, Nov. 1999.
- [17] D. Gesbert, H. Bölcskei, D. A. Gore, and A. J. Paulraj, "Outdoor MIMO wireless channels: Models and performance prediction," *IEEE Trans. Commun.*, vol. 50, no. 12, pp. 1926–1934, Dec. 2002.
- [18] A. Paulraj, private communication.
- [19] R. J. Muirhead, *Aspects of Multivariate Statistical Theory*. New York: Wiley, 1982.
- [20] A. M. Tulino and S. Verdú, "Random matrix theory and wireless communications," *Found. Trends Commun. Inf. Theory*, vol. 1, no. 1, Jun. 2004.
- [21] P. G. Moschopoulos, "The distribution of the sum of independent gamma random variables," *Ann. Inst. Statist. Math. (Part A)*, vol. 37, pp. 541–544, 1985.
- [22] M.-S. Alouini, A. Abdi, and M. Kaveh, "Sum of gamma variates and performance of wireless communication systems over Nakagami-fading channels," *IEEE Trans. Veh. Technol.*, vol. 50, no. 6, pp. 1471–1480, Nov. 2001.
- [23] T. F. Coleman and Y. Li, "On the convergence of reflective Newton methods for large-scale nonlinear minimization subject to bounds," *Math. Progr.*, vol. 67, no. 2, pp. 189–224, 1994.
- [24] P. E. Gill, W. Murray, and M. H. Wright, *Practical Optimization*. London, U.K.: Academic, 1981.
- [25] S. Alamouti, "A simple transmit diversity technique for wireless communications," *IEEE J. Sel. Areas Commun.*, vol. 16, pp. 1451–1458, Oct. 1998.
- [26] V. Tarokh, H. Jafarkhani, and A. R. Calderbank, "Space-time block codes from orthogonal designs," *IEEE Trans. Inf. Theory*, vol. 45, pp. 1456–1467, July 1999.
- [27] *TGn Channel Models*, IEEE 802.11 standard contribution 802.11-03/940r4.
- [28] B. Clerckx, "Space-Time Signaling for Real-World MIMO Channels," Ph.D. Dissertation, Université catholique de Louvain, Louvain, France, Sep. 2005.
- [29] S. Tavildar and P. Viswanath, "Approximately universal codes over slow fading channels," *IEEE Trans. Inf. Theory*, to be published.
- [30] S. Verdú, "Spectral efficiency in the wideband regime," *IEEE Trans. Inf. Theory*, vol. 48, no. 6, pp. 1319–1343, Jun. 2002.
- [31] S. Shamai and S. Verdú, "The impact of frequency-flat fading on the spectral efficiency of CDMA," *IEEE Trans. Inf. Theory*, vol. 47, no. 4, pp. 1302–1327, May 2001.
- [32] D. Guo, S. Shamai, and S. Verdú, "Mutual information and minimum mean-square error in Gaussian channels," *IEEE Trans. Inf. Theory*, vol. 51, no. 4, pp. 1261–1282, Apr. 2005.
- [33] H. Lutkepohl, *Handbook of Matrices*. Chichester, U.K.: Wiley, 1996.
- [34] G. Letac and H. Massam, A Tutorial on Noncentral Wishart Distributions 2004 [Online]. Available: <http://www.lsp.ups-tlse.fr/Fp/Letac/Wishartnoncentrales.pdf>